Title: BCAS2 promotes primitive hematopoiesis by sequestering β-catenin within the nucleus

Authors: Guozhu Ning[1,2#], Yu Lin[3#], Haixia Ma[4,5], Jiaqi Zhang[4,5], Liping Yang[1], Zhengyu Liu[1], Lei Li[4,5]*, Xinyu He[1]*, Qiang Wang[1]*

Affiliations:

[1]Innovation Centre of Ministry of Education for Development and Diseases, the Sixth Affiliated Hospital, School of Medicine, South China University of Technology, Guangzhou 510006, China

[2]Affiliated Hospital of Guangdong Medical University & Key Laboratory of Zebrafish Model for Development and Disease of Guangdong Medical University, Zhanjiang 524001, China

[3]School of Pharmacy, Qiqihar Medical University, Qiqihar 161006, China

[4]Institute State Key Laboratory of Stem Cell and Reproductive Biology, Institute of Stem Cell and Regeneration, Beijing Institute of Stem Cell and Regenerative Medicine, Institute of Zoology, Chinese Academy of Sciences, Beijing 100101, China.

[5]University of Chinese Academy of Sciences, Beijing 100049, China.

[#]These authors contributed equally.

*To whom correspondence should be addressed: (Lei Li) lil@ioz.ac.cn; (Xinyu He) hexyu@scut.edu.cn; (Qiang Wang) qiangwang@scut.edu.cn

Abstract

Breast carcinoma amplified sequence 2 (BCAS2), a core component of the hPrP19 complex, plays crucial roles in various physiological and pathological processes. However, whether BCAS2 has functions other than being a key RNA-splicing regulator within the nucleus remains unknown. Here, we show that BCAS2 is essential for primitive hematopoiesis in zebrafish and mouse embryos. The activation of Wnt/β-catenin signal, which is required for hematopoietic progenitor differentiation, is significantly decreased upon depletion of *bcas2* in zebrafish embryos and mouse embryonic fibroblasts (MEFs). Interestingly, BCAS2 deficiency has no obvious impact on the splicing efficiency of β-catenin pre-mRNA, while significantly attenuating β-catenin nuclear accumulation. Moreover, we find that BCAS2 directly binds to β-catenin via its coiled-coil domains, thereby sequestering β-catenin within the nucleus. Thus, our results uncover a previously unknown function of BCAS2 in promoting Wnt signaling by enhancing β-catenin nuclear retention during primitive hematopoiesis.

43 **Introduction**

44 Hematopoiesis refers to the lifelong process by which all blood cell lineages are
45 generated. It begins at the early stage of embryonic development, providing the
46 growing embryo with sufficient oxygen and nutrients.[1] Evolutionarily conserved
47 across vertebrate species, hematopoiesis consists of two successive and partially
48 overlapping waves: primitive and definitive. In mammals, the first wave of
49 hematopoiesis occurs in the yolk-sac blood islands, producing primitive erythroid,
50 megakaryocyte and macrophage progenitors, which can be observed in mouse
51 embryos as early as embryonic day 7.25 (E7.25).[2-4] In zebrafish, primitive
52 hematopoiesis initiates at around 11 hours post fertilization (hpf), when
53 hemangioblasts emerge from the anterior lateral mesoderm (ALM) and posterior
54 lateral mesoderm (PLM) and later differentiate into both hematopoietic and
55 endothelial cells.[5-7]

56 Breast cancer amplified sequence 2 (BCAS2), also known as pre-mRNA splicing
57 factor SPF27, is a 26-kDa nuclear protein containing two coiled-coil (CC) domains.[8]
58 It was initially found to be overexpressed and amplified in human breast cancer cell
59 lines.[9-11] Further studies have identified BCAS2 as a vital component of the human
60 Prp19/CDC5L complex, which forms the catalytic ribonucleoprotein (RNP) core of
61 spliceosome and is required for the activation of pre-mRNA splicing.[9,12,13] In
62 Drosophila, the function of BCAS2 in RNA splicing is essential for cell viability.[14] In
63 mouse, disruption of *Bcas2* in male germ cells impairs mRNA splicing and leads to a
64 failure of spermatogenesis.[15] Additionally, BCAS2 has been shown to be a negative

65 regulator of p53 by directly interacting with p53 or modulating alternative splicing of
66 *Mdm4*, a major p53 inhibitor.[8,16] Zebrafish *bcas2* transcripts were enriched in the sites
67 of both primitive and definitive hematopoiesis during embryonic development.[16]
68 However, a previous study showed that p53 overactivation induced by zebrafish
69 *bcas2* depletion did not affect primitive hematopoiesis, but impaired definitive
70 hematopoiesis.[16] In recent years, several studies have highlighted the importance of
71 regulating the expression and activity of p53 in primitive erythroid cell differentiation
72 in both mouse and zebrafish embryos.[17-19] Thus, it is necessary to reexamine the exact
73 function of BCAS2 in primitive hematopoiesis.

74 Wnt signaling, usually categorized into canonical and non-canonical pathways, is
75 involved in the process of hematopoiesis.[20-22] Notably, the canonical Wnt signaling
76 pathway, which is dependent on the nuclear accumulation of β-catenin to regulate
77 gene transcription, controls primitive hematopoietic progenitor formation and
78 promotes definitive hematopoietic stem cell (HSC) specification.[23-25] For instance, it
79 has been demonstrated in *Xenopus* that, Wnt4-mediated activation of Wnt/β-catenin
80 signaling plays a critical role in the induction and maintenance of primitive
81 hematopoiesis.[26] Moreover, transient inhibition of canonical Wnt signaling in
82 zebrafish embryos impairs embryonic blood formation.[27] However, previous studies
83 utilizing human pluripotent stem cells revealed an opposite role of Wnt/β-catenin
84 pathway in primitive progenitor generation.[25,28] Therefore, the impact of Wnt/β-
85 catenin signaling on primitive hematopoiesis remains elusive and even controversial.
86 Moreover, it has been suggested that BCAS2 is important for neural stem cell

87 proliferation and dendrite growth in mice by regulating β-catenin pre-mRNA
88 splicing.[29,30] As a nuclear protein, it is unclear whether BCAS2 can modulate Wnt/β-
89 catenin signaling in a splicing-independent manner.

90 In this study, we generated two zebrafish *bcas2* mutant lines, both of which
91 exhibited defects in male fertility and embryonic HSC formation, similar to what was
92 previously reported in mice and zebrafish.[15,16] More importantly, loss-of-function
93 experiments suggest that BCAS2 is necessary for primitive hematopoiesis in both
94 zebrafish and mouse embryos. We further find that *bcas2* is dispensable for the
95 survival and proliferation of hematopoietic cells, but plays a crucial role in the
96 differentiation of the hematopoietic lineage from hemangioblasts. Using a
97 comprehensive approach, we reveal that BCAS2 is a nuclear retention factor for β-
98 catenin during primitive hematopoiesis. Subsequent biochemical and functional
99 experiments demonstrate that BCAS2 directly binds to β-catenin and suppresses its
100 nuclear export to promote Wnt signal activation and hematopoietic progenitor
101 differentiation. Furthermore, the CC domains on BCAS2 and the Armadillo (ARM)
102 repeats on β-catenin are responsible for their interaction. Collectively, we have
103 uncovered a novel function of BCAS2 in regulating Wnt/β-catenin signaling by
104 sequestering β-catenin within the nucleus during primitive hematopoiesis.

105

106 **Methods**

107 **Animal models**

108 Our studies including animal maintenance and experiments were performed in

109 compliance with the guidelines of the Animal Care and Use Committee of the South
110 China University of Technology (Permission Number: 2023092). Seven strains of
111 zebrafish were used in this study, including Tübingen wild-type, *bcas2* mutant, *cloche*
112 mutant, *Tg(gata1:GFP)*, *Tg(coro1a:eGFP)*, *Tg(kdrl:GFP)*, and *Tg(hsp70l:dkk1b-*
113 *GFP)*. *cloche* mutant, *Tg(gata1:GFP)* and *Tg(kdrl:GFP)* lines were provided by
114 Professor Feng Liu (Chinese Academy of Sciences). *Tg(coro1a:eGFP)* was provided
115 by Professor Yiyue Zhang (South China University of Technology). *Tg(hsp70l:dkk1b-*
116 *GFP)* strain was purchased from China Zebrafish Resource Center. *Bcas2*$^{Floxed/Floxed}$
117 (*Bcas2*$^{F/F}$) mouse line was generated as previously described.[15] Genotyping of
118 *Bcas2*$^{F/F}$ mouse and *Flk1*-Cre mouse was performed using primers listed in
119 Supplemental Table 1. The mouse model with *Bcas2* specifically disrupted in the
120 hemangioblasts was derived from mating female *Bcas2*$^{F/F}$ mice with *Flk1*-Cre
121 transgenic mice. All mouse lines were maintained on a mixed background
122 (129/C57BL/6).
123

124 **Cell lines and transfection**

125 HEK293T, HeLa, SW480, and L cell lines were obtained from ATCC. Conditional
126 *Bcas2* knockout (*Bcas2*-cKO) mouse embryonic fibroblasts (MEFs) were prepared
127 from *Bcas2*$^{F/F}$ embryos at E13.5. Cells were cultured in Dulbecco's modified eagle's
128 medium (DMEM, HyClone) supplemented with 10% fetal bovine serum (FBS,
129 HyClone) and 1% penicillin-streptomycin (HyClone) at 37 °C and 5% CO_2. L cell
130 lines expressing Wnt3a were maintained under similar conditions in the presence of

131 400 μg/ml G-418, from which Wnt3a conditioned medium (Wnt3a CM) was
132 generated. Culture medium prepared from L-cells was used as a control. To stimulate
133 Wnt signaling, cells were treated with Wnt3a CM in a 1:1 ratio with normal media. To
134 deplete *Bcas2* expression, *Bcas2*-cKO MEFs were cultured in medium containing 2
135 μM tamoxifen for 72 h and the knockout efficiency was evaluated using western blot
136 analysis. The same cells cultured without tamoxifen were used as a control. To silence
137 *BCAS2* expression, shRNA constructs in pLL 3.7-GFP plasmid were generated to
138 target the following sequences: shRNA1, GAATGTGTAAACAATTCTA; shRNA2:
139 GAAGGAACTTCAGAAGTTA. Transfection was performed with Lipofectamine
140 2000 (11668019, Invitrogen) according to the manufacturer's instructions.
141
142 **Generation of CRISPR-Cas9-mediated *bcas2* knockout zebrafish**
143 The *bcas2* knockout zebrafish mutants were generated by CRISPR-Cas9 system as
144 previously described.[31] The guide RNA was designed to target the sequences 5′-
145 GGCGCAGCTGGAGCATCAGG-3′ within exon 4 of *bcas2*. Humanized Cas9
146 mRNA and gRNA were co-injected into wild-type embryos at the 1-cell stage.
147 Embryos or adult fin clips were collected to prepare genomic DNA. To screen for
148 mutant alleles, the genomic regions containing gRNA-targeted sequences were
149 amplified by polymerase chain reaction (PCR) with primers listed in Supplemental
150 Table 1. The PCR products were sequenced or digested with T7 endonuclease or
151 restriction enzyme FspI for genotyping.
152

153 **RNA, morpholinos, and microinjection**

154 Capped mRNAs for human *BCAS2*, *BCAS2 △CC1-2*, *BCAS2 CC1-2* and mouse *ΔN-*
155 *β-catenin* mRNA were synthesized from the corresponding linearized plasmids using
156 an mMESSAGE mMACHINE T7 transcription kit (AM1344, Ambion). Morpholinos
157 (MOs) were designed and purchased from Gene Tools: mismatch MO (cMO 5'-
158 AGCCACTCATCCTGCTCCTCCCATC-3'), and *bcas2* translation-blocking MO
159 (tMO; 5'-AGCGACTGATGCTGGTCCTGCCATC-3'). The mRNAs and
160 morpholinos were injected into embryos at the 1- to 2-cell stage.

161

162 **Whole-mount *in situ* hybridization**

163 Digoxigenin-labeled and fluorescein-labeled probes were synthesized using a RNA
164 Labeling kit (11175025910, Roche). Whole-mount *in situ* hybridization (WISH) and
165 double fluorescence *in situ* hybridization for zebrafish embryos were performed
166 following previously published methods.[32,33] Anti-digoxigenin-POD (11633716001,
167 Roche) and anti-fluorescein-POD (11426346910, Roche) were used to detect
168 digoxigenin-labeled probes and fluorescein-labeled probes, respectively. After WISH,
169 the stained embryos were embedded in OCT and sections were prepared with a
170 LEICA CM1900. The mouse yolk sac layers were separated as previously described.[34]

171

172 ***o*-Dianisidine staining**

173 To evaluate hemoglobin level, embryos were harvested at 36 hpf or 48 hpf, then
174 stained with *o*-dianisidine as previously described.[35]

175

176 **Proliferation and apoptosis assays**

177 Embryos were incubated with 10 mM bromodeoxyuridine (BrdU) (B5002, Sigma) for
178 20 min. The incorporated BrdU was detected with anti-BrdU (B2531, Sigma)
179 antibody. TUNEL staining was performed using *In Situ* Cell Death Detection Kit,
180 TMR red (12156792910, Roche) according to the manufacturer's recommendation.

181

182 **Heat shock treatment**

183 To induce *dkk1* expression, *Tg(hsp70l:dkk1b-GFP)* embryos were subjected to heat
184 shock (42°C) for 10 min at 10 hpf, and then collected at the indicated stage for WISH.

185

186 **Dual reporter assay**

187 HEK293T cells or MEFs were seeded in 24-well plates and transfected with a Super-
188 TOPflash plasmid containing multimerized TCF-binding elements and a Renilla
189 luciferase plasmid, along with the indicated vectors. Then cells were treated with 100
190 ng/mL LiCl and/or Wnt3a CM for 12 h and assayed for luciferase activity using the
191 Dual luciferase system (E1910, Promega).

192

193 **Immunoprecipitation, GST pulldown, and western blotting**

194 For immunoprecipitation, HEK293T cells were transfected with the indicated
195 plasmids and collected 48 h after transfection. Subsequently, HEK293T cells were
196 lysed in a lysis buffer (10 mM Tris-HCl, pH 7.5, 150 mM NaCl, 2 mM EDTA and

197 0.5% Nonidet P-40) containing protease inhibitors. Immunoprecipitation was
198 performed in accordance with the standard protocols.
199 For GST pulldown assay, GST, GST tagged β-catenin ARM 1-12 and His tagged
200 BCAS2 were expressed in *Escherichia coli* BL21, then purified using Glutathione-
201 Sepharose 4B beads (71024800-GE, GE Healthcare) and HisPur Ni-NTA beads
202 (88831, Thermo Fisher), respectively. GST and GST-β-catenin ARM 1-12 proteins
203 were immobilized onto Glutathione-Sepharose 4B beads and incubated with purified
204 His-BCAS2 at 4°C for 4 h. Beads were washed three times and analyzed using
205 western blotting.
206 Cytoplasmic and nuclear extracts were separated with nuclear and cytoplasmic
207 extraction kit (CW0199, CWBIO). Cell lysates were subjected to
208 immunoprecipitation with anti-Flag M2 affinity gel (A2220, Sigma) or anti-c-Myc
209 agarose affinity gel (A7470, Sigma) antibodies. Proteins were analyzed by western
210 blot using anti-Flag (F2555, Sigma), anti-HA (CW0092A, CWBIO), anti-β-catenin
211 (M24002, Abmart), anti-BCAS2 (10414-1-AP, Proteintech), anti- β -Tubulin
212 (CW0265A, CWBIO), anti-GFP (A11120, Thermo Fisher), anti-Histone H3 (ab1791,
213 Abcam), anti-GST (SAB4200237, Sigma), and anti-His Tag (AF5060, Beyotime)
214 antibodies.
215
216 **Immunofluorescence staining**
217 Cells on coverslips and embryos were processed for immunofluorescence staining as
218 previously described.[36,37] Before fixation, *bcas2*-deficient MEFs were treated with a

219 concentration of 20 μM MG132 or 20 nM leptomycin B (LMB) for 6 h, while
220 *Tg(gata1:GFP)* embryos were treated with 20 nM LMB from the bud stage to the 10-
221 somite stage. The prepared samples were stained with anti-BCAS2 (10414-1-AP,
222 Proteintech), anti-β-catenin (M24002, Abmart), and anti-GFP (A11122, Invitrogen).
223 Meanwhile, 4′,6-Diamidine-2′-phenylindole dihydrochloride (DAPI, 10236276001,
224 Sigma) was used to label nuclei. Fluorescence imaging was performed using a Nikon
225 A1R+ confocal microscope and all images were captured with the same settings. The
226 relative fluorescence intensity was calculated by dividing the fluorescence intensity of
227 nuclear β-catenin by the fluorescence intensity of DAPI.
228

229 **Bimolecular fluorescence complementation assay**

230 To construct the plasmids for Bimolecular fluorescence complementation assay
231 (BiFC), BCAS2 was fused to the N-terminal half of yellow fluorescent protein (YN-
232 BCAS2) and β-catenin to the C-terminal half (YC-β-catenin). YN-BCAS2 and YC-β-
233 catenin were either individually or collectively transfected into HeLa cells.
234 Fluorescence was detected 48 h after transfection using a Nikon A1R+confocal
235 microscope.
236

237 **Fluorescence recovery after photobleaching**

238 BCAS2 and GFP tagged S37A-β-catenin were co-transfected into HeLa cells.
239 Fluorescence recovery after photobleaching (FRAP) assay was performed according
240 to previously reported methods.[38] The cells were bleached by the 488 nm laser line of

241 the 20 mW argon laser at 100% power. About 90% of nuclear or cytoplasmic GFP
242 signal was bleached. Images were acquired with 35 frames at 25-s intervals by a
243 META Zeiss 510 confocal microscope.
244
245 **RNA sequencing**
246 Embryos were collected at the 10-somite stage and gently transferred into lysis buffer.
247 Reverse transcription was performed using a SMARTer Ultra Low RNA Kit
248 (Clontech, 634437) directly from the cell lysates. The cDNA library was prepared
249 using an Advantage 2 PCR Kit (Clontech， 639206) and then sequenced via the
250 Illumina sequencing platform (NovaSeq 6000). The difference in the number of
251 alternative splicing events between groups was analyzed using rMATS (version 4.1.0).
252
253 **Reverse transcription PCR**
254 Total RNA was isolated from wild-type and *bcas2* mutant embryos at the 10-somite
255 stage with MicroElute Total RNA kit (OMEGA, R6831-01), followed by reverse
256 transcription using ReverTra Ace qPCR RT Kit (Toyobo, FsQ-101). The cDNA was
257 amplified with primers listed in Supplemental Table 2.
258
259 **Quantification and statistical analysis**
260 Images were quantified with Image J. Statistical data were analyzed using Graph Pad
261 Prism. Comparisons between experimental groups were done using the Student's *t-test*.
262 Data are presented as mean ± standard deviation. $P < 0.05$, $P < 0.01$, $P < 0.001$, and P

263 < 0.0001 were considered statistically significant and marked with *, **, ***, and
264 ****, respectively (Student's *t-test*).
265
266 **Results**
267 **BCAS2 is necessary for primitive hematopoiesis**
268 To confirm that *bcas2* is expressed in the posterior intermediate cell mass (ICM)
269 where primitive hematopoiesis occurs in zebrafish, we first examined the
270 spatiotemporal expression pattern of *bcas2* during zebrafish embryo development by
271 performing whole mount *in situ* hybridization (WISH). The results showed that *bcas2*
272 was ubiquitously expressed from 1-cell stage to 10-somite stage (Supplemental Figure
273 1A). Its expression in the ICM became detectable at 18 hours post fertilization (hpf)
274 and was significantly elevated at 22 hpf (Figure 1A). We further observed that *bcas2*
275 was co-expressed with the primitive erythropoietic marker *gata1* in the ICM at 22 hpf
276 by fluorescence *in situ* hybridization (FISH) (Figure 1B). In contrast, *bcas2* was
277 hardly detectable in the ICM in *cloche*$^{-/-}$ mutants that lack both endothelial and
278 hematopoietic cells (Figure 1C). These results demonstrate a dynamic expression of
279 *bcas2* in the ICM and imply a potential role of this gene in primitive hematopoiesis.
280 To gain insight into the developmental function of *bcas2*, we employed
281 CRISPR/Cas9 system to generate *bcas2* mutants. Two mutant lines were obtained,
282 designated *bcas2*$^{\Delta 7}$ (with a 7-base deletion) and *bcas2*$^{\Delta 14}$ (with a 14-base deletion).
283 These mutations led to premature translation termination, which resulted in truncated
284 Bcas2 proteins lacking the C-terminal CC domains (Supplemental Figure 2A-B).

285 *bcas2*$^{+/\Delta 7}$ and *bcas2*$^{+/\Delta 14}$ mutants were identified by T7 endonuclease I assay or
286 restriction enzyme analysis (FspI) (Supplemental Figure 2C). We found that nearly
287 85% of the embryos derived from crossing *bcas*2$^{+/-}$ males with *bcas*2$^{+/-}$ females did
288 not develop to the cleavage stage (Supplemental Figure 2D). Only 3% of the living
289 embryos were homozygotes. In contrast, embryos obtained by crossing between wild-
290 type males and *bcas*2$^{+/-}$ females were viable and showed normal morphology, with a
291 heterozygosity rate consistent with Mendelian inheritance. This could be explained by
292 male infertility as previously documented in *Bcas2* knockout mice.[15] Combining the
293 above findings, we propose that Bcas2 may have an evolutionarily conserved role in
294 spermatogenesis.

295 Given the difficulty of obtaining homozygous mutants, embryos lacking one copy
296 of *bcas2* gene were produced from crosses between heterozygous females and wild-
297 type males. We observed a significant decrease of *bcas2* expression in the ICM region
298 in *bcas2*$^{+/\Delta 7}$ or *bcas2*$^{+/\Delta 14}$ mutants, likely resulting from nonsense-mediated RNA
299 decay (Figure 1D). In line with a previous report,[16] a marked reduction in the
300 expression of the HSC marker *cmyb* and T-cell marker *rag1* was found in *bcas2*$^{+/\Delta 7}$ or
301 *bcas2*$^{+/\Delta 14}$ embryos at 5 dpf, indicating an essential role of *bcas2* in definitive
302 hematopoiesis (Supplemental Figure 3A-B). These findings suggest that *bcas2*$^{+/\Delta 7}$ and
303 *bcas2*$^{+/\Delta 14}$ mutants can be used to examine the involvement of *bcas2* in primitive
304 hematopoiesis.

305 To explore whether *bcas2* is required for primitive hematopoiesis, we first
306 examined the expression of primitive erythropoietic markers *gata1* and *hbbe3* in

307 *bcas2*$^{+/\Delta 7}$ and *bcas2*$^{+/\Delta 14}$ embryos at 22 hpf, and observed a marked decrease in the
308 expression of these genes in the mutants (Figure 1E-F). Surprisingly, *o*-dianisidine
309 staining showed similar hemoglobin contents in the *bcas2*$^{+/\Delta 7}$ and *bcas2*$^{+/\Delta 14}$ embryos
310 at 48 hpf compared with control embryos, suggesting that the defect in primitive
311 hematopoiesis induced by haploinsufficiency of *bcas2* was alleviated at later
312 developmental stages. In order to further explore the role of BCAS2 in primitive
313 hematopoiesis, we identified several *bcas2*$^{\Delta 14/\Delta 14}$ mutants from about 100 embryos.
314 These homozygous mutants display a severe decrease in hemoglobin (Figure 1G).
315 Moreover, injection of a translation-blocking MO into wild-type embryos to
316 downregulate *bcas2* expression resulted in severe defects in erythropoiesis at 22 hpf
317 and 48 hpf (Supplemental Figure 4A-D). These results indicate that *bcas2* is
318 indispensable for primitive hematopoiesis in zebrafish. In addition, transgenic mice
319 expressing Cre recombinase under the control of the *Flk1* promoter were crossed to
320 *Bcas2*$^{F/F}$ animals to induce the deletion of *Bcas2* in endothelial/hematopoietic cells.
321 We found that red blood cells were eliminated in the yolk sac of *Bcas2*$^{F/F}$*;Flk1-Cre*
322 mice at E12.5 despite the presence of vessels (Figure 1H). Therefore, Bcas2 has a
323 conserved role in vertebrates to regulate primitive hematopoiesis.
324

325 ***bcas2* deficiency impairs hematopoietic progenitor differentiation**

326 The decrease of primitive hematopoietic cells in *bcas2* deficient animals may be
327 attributed to a number of possible causes: excessive apoptosis, hampered proliferation
328 of hematopoietic cells, or impaired differentiation of hematopoietic progenitor cells.

329 To shed light on this issue, we first performed terminal deoxynucleotidyl transferase-
330 mediated dUTP nick end labeling (TUNEL) assay in *Tg(gata1:GFP)* embryos at the
331 10-somite stage to examine DNA fragmentations in apoptotic cells, and found no
332 obvious apoptotic signal in the *gata1*$^{+}$ hematopoietic cells in either *bcas2*$^{+/\Delta 14}$
333 embryos or their wild-type siblings (Supplemental Figure 5A). Meanwhile, BrdU
334 incorporation assay revealed no significant difference in hematopoietic cell
335 proliferation between *bcas2*$^{+/\Delta 14}$ mutants and their corresponding wild-types
336 (Supplemental Figure 5B-C). These data suggest that *bcas2* is dispensable for the
337 survival and proliferation of hematopoietic cells.

338 In the developing embryo, hemangioblasts are derived from the ventral mesoderm
339 at early somite stage, and then differentiate into both hematopoietic and endothelial
340 lineages.[39,40] To test whether *bcas2* functions in cell fate decision during primitive
341 hematopoietic cell development, the expression of hemangioblast markers *npas4l*, *scl*,
342 and *gata2* in *bcas2*$^{+/\Delta 14}$ embryos was examined at the 1- to 2-somite stage. As shown
343 in Figure 2A, haploinsufficiency of *bcas2* did not affect the emergence of the
344 hemangioblast population. Then we extended our analysis to include the markers of
345 hematopoietic and endothelial progenitors. Consistent with the decrease in primitive
346 hematopoietic cells in *bcas2* deficient mutants, a marked reduced expression of
347 erythrocyte progenitor markers *gata1* and *hbbe3* was observed in the posterior lateral
348 mesoderm of *bcas2*$^{+/-}$ embryos at the 10-somite stage (Figure 2B). Interestingly, the
349 expression of myeloid progenitor marker *pu.1* was also dramatically decreased
350 (Figure 2C). Moreover, overexpression of human BCAS2 enhanced the expression of

351 *gata1* in both wild-type and mutant embryos at the 10-somite stage (Figure 2D). In
352 contrast, the endothelial progenitor marker *fli1a* was expressed at a similar level in
353 *bcas2*$^{+/-}$ embryos as in wild-type animals (Figure 2E). Consistently, blood vessels
354 appeared normal in *bcas2*$^{+/-}$ mutants with *Tg(kdrl:GFP)* background at 54 hpf (Figure
355 2F). These data provide convincing evidence that *bcas2* is required for the
356 differentiation of the hematopoietic lineage from hemangioblasts during primitive
357 hematopoiesis.
358
359 **BCAS2 functions in primitive hematopoiesis by activating Wnt signaling**
360 Previous studies have shown that Wnt/β-catenin plays a key role in primitive
361 hematopoiesis.[26,27,41] As both BCAS2 and β-catenin-like 1 (CTNNBL1) are members
362 of the Prp19/CDC5L complex, which is a major building block of the spliceosome's
363 catalytic RNP core,[13] we speculate that BCAS2 may be a regulator of Wnt signaling
364 through interaction with β-catenin during hematopoiesis. To test our hypothesis,
365 human BCAS2 was overexpressed in HEK293T cells and MEFs. Ectopic expression
366 of BCAS2 enhanced the Wnt3a-induced expression of the TOPflash luciferase
367 reporter in a dose-dependent manner (Figure 3A-B). Importantly, Wnt3a-induced
368 luciferase activity in HEK293T cells could be effectively reduced by knockdown of
369 *BCAS2* using two shRNAs targeting different regions of human *BCAS2* (Figure 3C
370 and Supplemental Figure 6). Similar results were also observed in *Bcas2*-cKO MEFs
371 in the presence of tamoxifen (Figure 3D). Furthermore, the expression of *cdx4* and
372 *hoxa9a*, which are targets of canonical Wnt signaling in the regulation of

373 hematopoietic development,[42,43] were downregulated in the lateral plate mesoderm of
374 *bcas2*$^{+/-}$ embryos at the 6-somite stage (Supplemental Figure 7). These findings
375 support that BCAS2 promotes Wnt signaling activation.

376 To confirm that Wnt signaling was required for zebrafish embryonic hematopoiesis,
377 we induced the expression of canonical Wnt inhibitor Dkk1 by heat-shocking
378 *Tg(hsp70l:dkk1-GFP)*^{w32} embryos at the bud stage.[44] As expected, diminished
379 expression of *gata1* and *hbbe3* was detected in the resulting embryos at the 10-somite
380 stage (Figure 3E-F). In addition, treatment with a small molecule β-catenin antagonist
381 CCT036477 from 9 hpf did not affect the expression of hemangioblast markers
382 *npas4l*,[45] *scl*, and *gata2* or endothelial marker *fli1a* (Supplemental Figure 8A-B), yet
383 significantly reduced the expression of erythroid progenitor marker *gata1* in wild-type
384 embryos (Supplemental Figure 8C), suggesting that canonical Wnt signaling may not
385 be required for the generation of hemangioblasts or their endothelial differentiation,
386 but is pivotal for their hematopoietic differentiation. To further validate that *bcas2*
387 functions in primitive hematopoiesis via Wnt/β-catenin signaling, the expression
388 pattern of β-catenin was examined in *bcas2* morphants with *Tg(gata1:GFP)*
389 background at the 10-somite stage by immunofluorescent staining. The signal of
390 nuclear β-catenin was substantially decreased in hematopoietic progenitor cells
391 (Figure 3G-H) and primitive myeloid cells (Supplemental Figure 9A-B). Moreover,
392 overexpression of ΔN-β-catenin, a constitutively active form of β-catenin, effectively
393 restored the expression of *hbbe3* in *bcas2* morphants and mutants (Figure 3I-J). All
394 these data suggest that BCAS2 functions in primitive hematopoiesis by regulating

395 Wnt/β-catenin signaling.

396

397 **BCAS2 promotes β-catenin nuclear accumulation independently of protein**

398 **stability regulation**

399 To investigate how BCAS2 regulates Wnt/β-catenin signaling, HEK293T cells were

400 treated with LiCl, a canonical Wnt agonist that inhibits GSK-3β activity and stabilizes

401 cytosolic β-catenin.[46] The results showed that TOPflash activity was significantly

402 elevated in LiCl-treated cells (Figure 4A). BCAS2 overexpression further upregulated,

403 whereas shRNA-mediated knockdown of *BCAS2* downregulated LiCl-induced

404 TOPflash activity (Figure 4A-B). Likewise, HEK293T cells transfected with S37A-β-

405 catenin, a constitutively active form of β-catenin that is resistant to GSK-3β-mediated

406 degradation, [47] displayed a much higher level of TOPflash activity, which was reduced

407 by *BCAS2* knockdown (Figure 4C). These results strongly imply that BCAS2

408 regulates Wnt signaling downstream of β-catenin stability control.

409 To test the above hypothesis, we evaluated nuclear β-catenin level by performing

410 immunofluorescence staining and immunoblotting experiments. Upon tamoxifen

411 exposure, nuclear accumulation of β-catenin induced by LiCl was greatly inhibited in

412 *Bcas2*-cKO MEFs, while nuclear/cytoplasmic fractionation suggested that

413 cytoplasmic β-catenin level remained relatively unchanged (Figure 4D-E). Similarly,

414 silencing *BCAS2* with shRNA led to reduced nuclear β-catenin in the human colon

415 cancer cell line SW480, in which β-catenin was activated because of mutations in the

416 adenomatous polyposis coli protein (APC), an integral component of the β-catenin

417 destruction complex (Figure 4F).[48] Next, MG132, a proteasome inhibitor, was applied
418 to activate Wnt/β-catenin signaling in *Bcas2*-cKO MEFs by inhibiting β-catenin
419 degradation. In the absence of tamoxifen and MG132, endogenous β-catenin was
420 localized almost exclusively in the cytoplasm; MG132 treatment dramatically
421 triggered β-catenin accumulation in the nuclei (Figure 4G). However, in *Bcas2*-cKO
422 MEFs exposed to tamoxifen, MG132 treatment was not able to induce nuclear
423 accumulation of β-catenin (Figure 4G). These findings indicate that BCAS2 promotes
424 β-catenin nuclear accumulation in a manner that is independent of β-catenin stability
425 regulation.
426
427 **BCAS2 sequesters β-catenin within the nucleus**
428 In addition to be affected by protein stability, the nuclear level of β-catenin is also
429 fine-tuned by the opposing actions of nuclear export and import.[49-51] To examine the
430 effect of BCAS2 on the nuclear import and export of β-catenin, fluorescent recovery
431 after photobleaching (FRAP) experiments was carried out in HeLa cells expressing
432 GFP-tagged S37A-β-catenin. After photobleaching the nucleus, no significant
433 difference was found in the recovery of nuclear GFP signals between the cells with
434 and without overexpression of BCAS2 (Supplemental Figures 10A, A', and C),
435 suggesting that BCAS2 does not regulate β-catenin nuclear import. Conversely, after
436 photobleaching the cytoplasm, BCAS2 overexpressed cells showed a much slower
437 recovery of cytoplasmic fluorescence (Supplemental Figures 10B, B', and C),
438 indicating that BCAS2 inhibits β-catenin nuclear export.

439 It has been suggested that the nuclear exit of β-catenin can be either dependent or
440 independent on CRM1, a major nuclear export receptor.[52] To shed light on the
441 mechanism underlying BCAS2 mediated β-catenin nuclear retention, we treated
442 *Bcas2*-cKO MEFs with the CRM1-specific export inhibitor LMB.[53] Regardless of the
443 presence or absence of endogenous BCAS2, LMB treatment could effectively
444 increase the level of β-catenin in the nucleus (Figure 5A). Consistently, treatment of
445 LMB was able to rescue the impaired nuclear accumulation of β-catenin in BCAS2-
446 deficient SW480 cells (Figure 5B). Moreover, when *bcas2* morphants in *Tg*
447 *(gata1:GFP)* background were treated with LMB from bud stage to 10 somite stage,
448 the level of nuclear β-Catenin was partially recovered (Figure 5C-D). Importantly, the
449 expression of *gata1* was also restored in *bcas2* mutants upon LMB treatment (Figure
450 5E). We further tested if BCAS2 specifically regulates CRM1-mediated nuclear
451 export of β-catenin by analyzing the nucleocytoplasmic distribution of other known
452 CRM1 cargoes, such as ATG3 and CDC37L.[54] Intriguingly, BCAS2 overexpression in
453 HeLa cells only slightly enhanced the nuclear localization of CDC37L, and had no
454 significant impact on that of ATG3 (Supplemental Figure 11), indicating the
455 specificity of BCAS2-mediated inhibition of CRM1-dependent nuclear export of β-
456 catenin. Taken together, these findings suggest that BCAS2 negatively regulates
457 CRM1-mediated nuclear export of β-catenin.
458
459 **BCAS2 directly interacts with β-catenin in the nucleus**
460 To investigate whether BCAS2 inhibits the nuclear export of β-catenin through

461 physical binding, HEK293T cells were transfected with Flag-tagged β-catenin and
462 HA-tagged BCAS2 constructs. Co-immunoprecipitation (Co-IP) experiments showed
463 that Flag-β-catenin was precipitated with HA-BCAS2 as well as endogenous BCAS2,
464 indicating an interaction between these two proteins (Figure 6A-B). In addition, the
465 interaction was enhanced upon Wnt3a stimulation (Figure 6C). Given that Wnt ligand
466 stimulation ultimately induces β-catenin nuclear accumulation, this enhanced
467 interaction implies that BCAS2 associates with β-catenin within the nucleus.
468 Therefore, we performed the bimolecular fluorescence complementation (BiFC) assay
469 to visualize the interaction of BCAS2 and β-catenin in living cells. In this assay, the
470 N-terminal fragment of yellow fluorescent protein (YFP) was fused to BCAS2 (YN-
471 BCAS2), while the C-terminal fragment was fused to β-catenin (YC-β-catenin)
472 (Figure 6D). As expected, the YFP fluorescence was specifically observed in the
473 nucleus (Figure 6E).

474 Previous studies have divided the β-catenin protein into three distinct domains,
475 including the N-terminal domain (residues 1–133), the central domain with 12 ARM
476 repeats (residues 134–670), and the C-terminal domain (residues 671–781).[55] To
477 identify the BCAS2 binding site, constructs expressing various truncated forms of β-
478 catenin were generated and co-transfected with BCAS2 into HEK293T cells (Figure
479 6F). Co-IP assays revealed that deletion of the N-terminal or C-terminal domain of β-
480 catenin did not alter the interaction between β-catenin and BCAS2 (Figure 6G). In
481 contrast, when the ARM repeats 1-12 of β-catenin were deleted, the resulting deletion
482 mutant showed virtually no interaction with BCAS2 (Figure 6G). GST pull-down

483 assay also demonstrated a direct interaction between BCAS2 and the ARM repeats of
484 β-catenin (Figure 6H). These results indicate that BCAS2 physically binds to the
485 ARM repeats of β-catenin. Furthermore, we found that the ARM repeats 9-12, but not
486 1-8, bound to BCAS2 (Figure 6G).

487 Transcriptional activation of the canonical Wnt target genes depends on β-catenin
488 nuclear localization and its physical association with TCF/LEF family members. As
489 the binding sites for TCF have been located in the ARM repeats 3-10 of β-catenin,[56] it
490 is likely that BCAS2-mediated nuclear sequestration of β-catenin through interacting
491 with the ARM repeats 9-12 would be compatible with the initiation of gene
492 transcription by allowing for the association of β-catenin and TCF. To validate this
493 possibility, co-IP assays were performed and we found that β-catenin still bound with
494 TCF4 in the presence of BCAS2 (Supplemental Figure 12), confirming that the
495 binding of BCAS2 to β-catenin would not interfere with the formation of β-
496 catenin/TCF complex.

497

498 **BCAS2 enhances β-catenin nuclear accumulation through its CC domains**

499 To determine which domain of BCAS2 binds to β-catenin, we constructed a series of
500 deletion mutants of BCAS2 (Figure 7A). Notably, we observed that among these
501 truncated mutants, only the one lacking both CC1 and CC2 domains lost the ability to
502 interact with β-catenin (Figure 7B). Moreover, these two CC domains alone or
503 together could interact with β-catenin (Figure 7C). Therefore, we conclude that
504 BCAS2 binds to β-catenin via its CC domains.

505 We next examined whether the CC domains are required for BCAS2 to promote
506 Wnt/β-catenin signaling. As shown in Figure 7D, overexpression of BCAS2 without
507 the CC domains failed to increase LiCl-induced TOPflash activity in HEK-293T cells.
508 Likewise, overexpression of the full-length or the CC domains alone, but not BCAS2
509 lacking the CC domains, restored the nuclear accumulation of β-catenin in *bcas2*
510 morphants (Figure 7E-F and Supplemental Figure 13A-B). The expression of *gata1* in
511 *bcas2* mutants was also recovered by overexpression of the full-length BCAS2, but
512 not the truncated form without the CC-domains (Figure 7G). Collectively, these
513 findings indicate that BCAS2 positively regulates Wnt signaling through sequestering
514 β-catenin within the nucleus via its CC domains during primitive hematopoiesis.

515 As BCAS2 is involved in the Prp19-CDC5L spliceosome complex that regulates
516 RNA splicing during spermiogenesis, neurogenesis, and definitive hematopoiesis,[15,16]
517 we wondered if this protein participates in primitive hematopoiesis via mRNA
518 alternative splicing. To this end, we performed RNA sequencing of 10-somite stage
519 embryos to identify abnormal events in alternative splicing in *bcas2*$^{+/\Delta 14}$ mutants.
520 However, upon haploinsufficiency of *bcas2*, neither the number of five major types of
521 alternative splicing events, nor the typical forms of alternative splicing were
522 significantly affected (Supplemental Figure 14A-B). Additionally, haploinsufficiency
523 of *bcas2* did not result in the alternative splicing of *mdm4* that predisposes cells to
524 undergo p53-mediated apoptosis in definitive hematopoiesis, as reported previously
525 by Yu *et al.* (Supplemental Figure 14C).[16,57] Furthermore, the splicing efficiency of β-
526 catenin pre-mRNA remained almost unchanged in *bcas2*$^{+/\Delta 14}$ mutants (Supplemental

527 Figure 14D). These results demonstrate that the defects in primitive hematopoiesis of
528 *bcas2*$^{+/\Delta 14}$ mutants are independent of the regulatory role of Bcas2 in pre-mRNA
529 splicing.
530

531 **Discussion**

532 BCAS2 is a 26-kDa nuclear protein involved in a multitude of developmental
533 processes, such as Drosophila wing development, dendritic growth, and
534 spermatogenesis.[8,14,15,58-60] In our study, we generated *bcas2* knockout zebrafish. The
535 heterozygotes not only showed male infertility, resembling the phenotype of *Bcas2*
536 germ cell-specific knockout mice reported previously,[15] but also exhibited impaired
537 definitive hematopoiesis, consistent with the earlier study.[16] Importantly, we found a
538 marked decrease in the expression of the primitive erythroid progenitor markers *gata1*
539 and *hbbe3* in these heterozygous mutants, which was rescued by overexpression of
540 BCAS2. Moreover, the defective primitive hematopoiesis in mutant zebrafish was
541 phenocopied in hemangioblast-specific *Bcas2* knockout mice. While the reason(s) for
542 the discrepancy between our data and the observations made by Yu *et al.* regarding the
543 role of *bcas2* in the development of primitive erythroid and myeloid cells remains to
544 be determined,[16] our findings in zebrafish and mouse embryos provide solid evidence
545 that BCAS2 plays a conserved role in primitive hematopoiesis.

546 As demonstrated in previous studies, BCAS2 is involved in various developmental
547 events by regulating pre-mRNA splicing.[14-16,29,30] However, our data showed that
548 haploinsufficiency of *bcas2* did not affect alternative splicing during primitive

549 hematopoiesis. These results imply that one copy of the *bcas2* gene is sufficient to
550 support mRNA splicing in zebrafish. Instead, we find that Bcas2 promotes primitive
551 hematopoiesis by sequestering β-catenin within the nucleus. It has been reported that
552 the *bcas2* deletion in zebrafish embryos induces alternative splicing of *Mdm4* that
553 predisposes cells to undergo p53-mediated apoptosis in HSPCs during definitive
554 hematopoiesis.[16] Intriguingly, we found that the loss of one copy of *bcas2* gene in
555 zebrafish also resulted in severe impairment of HSPCs and their derivatives. It is
556 possible that Bcas2 might also have a role in definitive hematopoiesis independent of
557 its splicing regulatory function.

558 For the past decades, given the contradictory conclusions obtained from various *in*
559 *vitro* and *in vivo* studies, the function of Wnt/β-catenin signaling in primitive
560 hematopoiesis remains elusive and controversial.[25-28] In the present study, we have
561 provided several lines of evidence supporting that Wnt/β-catenin signaling positively
562 regulates primitive hematopoiesis: (1) Inhibition of Wnt/β-catenin by overexpression
563 of the canonical Wnt inhibitor Dkk1 disrupts the formation of erythrocyte progenitors
564 at the 10-somite stage. (2) Defects in primitive hematopoiesis in *bcas2* morphants and
565 mutants are readily restored by overexpression of ΔN-β-catenin, a constitutively
566 active β-catenin. (3) Overexpression of the full-length BCAS2, but not the CC
567 domain-deleted BCAS2, restores the formation of the primitive erythroid progenitor
568 in *bcas2* mutants. (4) BCAS2 overexpression enhances the development of primitive
569 blood cells in wild-type embryos. All these data suggest that BCAS2-mediated Wnt/β-
570 catenin signal activation is necessary for primitive hematopoiesis.

571 In addition, Wnt/β-catenin signaling has been known as an important pathway
572 involved in the regulation of axis determination and neural patterning during
573 gastrulation.[61-64] In our study, neither the heterozygous *bcas2* mutant embryos nor the
574 very few homozygous ones, exhibited any morphological defects typically associated
575 with inhibition of Wnt signaling, such as ventralization or brain anteriorization. This
576 may be due to the presence of maternal Bcas2 in heterozygous and homozygous
577 mutant embryos which were derived from crossing *bcas2*$^{+/-}$ males with *bcas2*$^{+/-}$
578 females.

579 CRM1 can facilitate β-catenin nuclear export in distinct ways.[65] For example,
580 CRM1 usually recognizes and binds with the nuclear export signal (NES) sequences
581 in chaperon proteins, such as APC, Axin and Chibby,[66-68] to mediate the nuclear
582 export of β-catenin. On the other hand, CRM1 can also bind directly to and function
583 as an efficient nuclear exporter for β-catenin.[69] Since BCAS2 has not been reported to
584 contain any recognizable NES sequences, it will be interesting to investigate whether
585 BCAS2 competitively inhibits β-catenin from associating with CRM1, or with the
586 chaperone proteins.

587 In summary, we uncover a novel role of BCAS2 in primitive hematopoiesis
588 through enhancing nuclear retention of β-catenin. Our study provides new insights
589 into the mechanism of BCAS2-mediated Wnt signal activation during primitive
590 hematopoiesis. Given that BCAS2 and Wnt signaling are well documented to
591 contribute to cancer development,[70-74] it is appealing to further explore whether our
592 findings can be applied to future cancer research.

Acknowledgements

We acknowledge the financial support of the National Natural Science Foundation of China (32025014 and 32330029) and the National Key Research and Development Program of China (2018YFA0800200 and 2020YFA0804000).

Author Contributions

Guozhu Ning: Writing - Original draft, Visualization, Software, Methodology, Investigation, Formal analysis, Data curation, Conceptualization**. Yu Lin:** Visualization, Software, Methodology, Investigation, Formal analysis, Data curation**. Haixia Ma, Jiaqi Zhang, Liping Yang, Zhengyu Liu:** Methodology, Validation**. Lei Li:** Resources**. Xinyu He:** Writing - Review & Editing**. Qiang Wang:** Project administration, Supervision, Funding acquisition**.**

Conflict-of-interest disclosure

The authors declare no competing financial interests.

Additional files

Supplemental Figures

Supplemental Table 1

Supplemental Table 2

615 **References**

616 1. Galloway JL, Zon LI. Ontogeny of hematopoiesis: examining the emergence of
617 hematopoietic cells in the vertebrate embryo. *Curr Top Dev Biol*. 2003;53:139-158.
618 2. Murry CE, Keller G. Differentiation of embryonic stem cells to clinically relevant
619 populations: lessons from embryonic development. *Cell*. 2008;132(4):661-680.
620 3. Ferkowicz MJ, Yoder MC. Blood island formation: longstanding observations
621 and modern interpretations. *Exp Hematol*. 2005;33(9):1041-1047.
622 4. Palis J. Hematopoietic stem cell-independent hematopoiesis: emergence of
623 erythroid, megakaryocyte, and myeloid potential in the mammalian embryo. *FEBS*
624 *Lett*. 2016;590(22):3965-3974.
625 5. Paik EJ, Zon LI. Hematopoietic development in the zebrafish. *Int J Dev Biol*.
626 2010;54(6-7):1127-1137.
627 6. Detrich HW, 3rd, Kieran MW, Chan FY, et al. Intraembryonic hematopoietic cell
628 migration during vertebrate development. *Proc Natl Acad Sci U S A*.
629 1995;92(23):10713-10717.
630 7. Leung AY, Mendenhall EM, Kwan TT, et al. Characterization of expanded
631 intermediate cell mass in zebrafish chordin morphant embryos. *Dev Biol*.
632 2005;277(1):235-254.
633 8. Kuo PC, Tsao YP, Chang HW, et al. Breast cancer amplified sequence 2, a novel
634 negative regulator of the p53 tumor suppressor. *Cancer Res*. 2009;69(23):8877-8885.
635 9. Neubauer G, King A, Rappsilber J, et al. Mass spectrometry and EST-database
636 searching allows characterization of the multi-protein spliceosome complex. *Nature*

637 *Genetics*. 1998;20(1):46-50.

638 10. Nagasaki K, Maass N, Manabe T, et al. Identification of a novel gene, DAM1,
639 amplified at chromosome 1p13.3-21 region in human breast cancer cell lines. *Cancer*
640 *Letters*. 1999;140(1-2):219-226.

641 11. Qi C, Zhu YT, Chang J, Yeldandi AV, Rao MS, Zhu YJ. Potentiation of estrogen
642 receptor transcriptional activity by breast cancer amplified sequence 2. *Biochem*
643 *Biophys Res Commun*. 2005;328(2):393-398.

644 12. Ajuh P, Kuster B, Panov K, Zomerdijk JC, Mann M, Lamond AI. Functional
645 analysis of the human CDC5L complex and identification of its components by mass
646 spectrometry. *EMBO J*. 2000;19(23):6569-6581.

647 13. Grote M, Wolf E, Will CL, et al. Molecular architecture of the human
648 Prp19/CDC5L complex. *Mol Cell Biol*. 2010;30(9):2105-2119.

649 14. Chen PH, Lee CI, Weng YT, et al. BCAS2 is essential for Drosophila viability
650 and functions in pre-mRNA splicing. *RNA*. 2013;19(2):208-218.

651 15. Liu W, Wang F, Xu Q, et al. BCAS2 is involved in alternative mRNA splicing in
652 spermatogonia and the transition to meiosis. *Nat Commun*. 2017;8:14182.

653 16. Yu S, Jiang T, Jia D, et al. BCAS2 is essential for hematopoietic stem and
654 progenitor cell maintenance during zebrafish embryogenesis. *Blood*.
655 2019;133(8):805-815.

656 17. Bissinger R, Lang E, Gonzalez-Menendez I, et al. Genetic deficiency of the
657 tumor suppressor protein p53 influences erythrocyte survival. *Apoptosis*. 2018;23(11-
658 12):641-650.

659 18. Yang S, Cao S, Xu X, et al. adducin 1 is essential for the survival of erythroid
660 precursors via regulating p53 transcription in zebrafish. *iScience*. 2023;26(9):107516.
661 19. Stanic K, Reig G, Figueroa RJ, et al. The Reprimo gene family member, reprimo-
662 like (rprml), is required for blood development in embryonic zebrafish. *Sci Rep*.
663 2019;9(1):7131.
664 20. Richter J, Traver D, Willert K. The role of Wnt signaling in hematopoietic stem
665 cell development. *Critical Reviews in Biochemistry and Molecular Biology*.
666 2017;52(4):414-424.
667 21. Krimpenfort RA, Nethe M. Canonical Wnt: a safeguard and threat for
668 erythropoiesis. *Blood Advances*. 2021;5(18):3726-3735.
669 22. Kokolus K, Nemeth MJ. Non-canonical Wnt signaling pathways in hematopoiesis.
670 *Immunologic Research*. 2010;46(1-3):155-164.
671 23. Tarafdar A, Dobbin E, Corrigan P, Freeburn R, Wheadon H. Canonical Wnt
672 signaling promotes early hematopoietic progenitor formation and erythroid
673 specification during embryonic stem cell differentiation. *PLoS One*.
674 2013;8(11):e81030.
675 24. Nostro MC, Cheng X, Keller GM, Gadue P. Wnt, activin, and BMP signaling
676 regulate distinct stages in the developmental pathway from embryonic stem cells to
677 blood. *Cell Stem Cell*. 2008;2(1):60-71.
678 25. Sturgeon CM, Ditadi A, Awong G, Kennedy M, Keller G. Wnt signaling controls
679 the specification of definitive and primitive hematopoiesis from human pluripotent
680 stem cells. *Nature Biotechnology*. 2014;32(6):554-+.

681 26. Tran HT, Sekkali B, Van Imschoot G, Janssens S, Vleminckx K. Wnt/beta-catenin
682 signaling is involved in the induction and maintenance of primitive hematopoiesis in
683 the vertebrate embryo. *Proc Natl Acad Sci U S A*. 2010;107(37):16160-16165.
684 27. Lengerke C, Schmitt S, Bowman TV, et al. BMP and Wnt specify hematopoietic
685 fate by activation of the Cdx-Hox pathway. *Cell Stem Cell*. 2008;2(1):72-82.
686 28. Paluru P, Hudock KM, Cheng X, et al. The negative impact of Wnt signaling on
687 megakaryocyte and primitive erythroid progenitors derived from human embryonic
688 stem cells. *Stem Cell Research*. 2014;12(2):441-451.
689 29. Chen HH, Lu HY, Chang CH, et al. Breast carcinoma-amplified sequence 2
690 regulates adult neurogenesis via β-catenin. *Stem Cell Research & Therapy*.
691 2022;13(1).
692 30. Huang CW, Chen YW, Lin YR, et al. Conditional Knockout of Breast Carcinoma
693 Amplified Sequence 2 (BCAS2) in Mouse Forebrain Causes Dendritic Malformation
694 via β-catenin. *Scientific Reports*. 2016;6.
695 31. Chang N, Sun C, Gao L, et al. Genome editing with RNA-guided Cas9 nuclease
696 in zebrafish embryos. *Cell Res*. 2013;23(4):465-472.
697 32. Jia S, Ren Z, Li X, Zheng Y, Meng A. smad2 and smad3 are required for
698 mesendoderm induction by transforming growth factor-beta/nodal signals in zebrafish.
699 *J Biol Chem*. 2008;283(4):2418-2426.
700 33. Welten MC, de Haan SB, van den Boogert N, et al. ZebraFISH: fluorescent in situ
701 hybridization protocol and three-dimensional imaging of gene expression patterns.
702 *Zebrafish*. 2006;3(4):465-476.

703 34. Wallingford MC, Giachelli CM. Loss of PiT-1 results in abnormal endocytosis in
704 the yolk sac visceral endoderm. *Mech Dev*. 2014;133:189-202.
705 35. Lieschke GJ, Oates AC, Crowhurst MO, Ward AC, Layton JE. Morphologic and
706 functional characterization of granulocytes and macrophages in embryonic and adult
707 zebrafish. *Blood*. 2001;98(10):3087-3096.
708 36. Wei S, Dai MM, Liu ZT, et al. The guanine nucleotide exchange factor Net1
709 facilitates the specification of dorsal cell fates in zebrafish embryos by promoting
710 maternal β-catenin activation. *Cell Research*. 2017;27(2):202-225.
711 37. Yang SY, Ning GZ, Hou YM, et al. Myoneurin regulates BMP signaling by
712 competing with Ppm1a for Smad binding. *Iscience*. 2022;25(6).
713 38. Schmierer B, Hill CS. Kinetic analysis of Smad nucleocytoplasmic shuttling
714 reveals a mechanism for transforming growth factor beta-dependent nuclear
715 accumulation of Smads. *Mol Cell Biol*. 2005;25(22):9845-9858.
716 39. Vogeli KM, Jin SW, Martin GR, Stainier DY. A common progenitor for
717 haematopoietic and endothelial lineages in the zebrafish gastrula. *Nature*.
718 2006;443(7109):337-339.
719 40. Reischauer S, Stone OA, Villasenor A, et al. Cloche is a bHLH-PAS transcription
720 factor that drives haemato-vascular specification. *Nature*. 2016;535(7611):294-298.
721 41. Sun H, Wang Y, Zhang J, et al. CFTR mutation enhances Dishevelled degradation
722 and results in impairment of Wnt-dependent hematopoiesis. *Cell Death Dis*.
723 2018;9(3):275.
724 42. Pilon N, Oh K, Sylvestre JR, Bouchard N, Savory J, Lohnes D. is a direct target

725 of the canonical Wnt pathway. *Developmental Biology*. 2006;289(1):55-63.

726 43. Sun HQ, Wang Y, Zhang JT, et al. CFTR mutation enhances Dishevelled
727 degradation and results in impairment of Wnt-dependent hematopoiesis. *Cell Death &*
728 *Disease*. 2018;9.

729 44. Stoick-Cooper CL, Weidinger G, Riehle KJ, et al. Distinct Wnt signaling
730 pathways have opposing roles in appendage regeneration. *Development*.
731 2007;134(3):479-489.

732 45. Krause U, Ryan DM, Clough BH, Gregory CA. An unexpected role for a Wnt-
733 inhibitor: Dickkopf-1 triggers a novel cancer survival mechanism through modulation
734 of aldehyde-dehydrogenase-1 activity. *Cell Death & Disease*. 2014;5.

735 46. Meijer L, Skaltsounis AL, Magiatis P, et al. GSK-3-selective inhibitors derived
736 from Tyrian purple indirubins. *Chem Biol*. 2003;10(12):1255-1266.

737 47. Easwaran V, Song V, Polakis P, Byers S. The ubiquitin-proteasome pathway and
738 serine kinase activity modulate adenomatous polyposis coli protein-mediated
739 regulation of beta-catenin-lymphocyte enhancer-binding factor signaling. *J Biol Chem*.
740 1999;274(23):16641-16645.

741 48. Rosin-Arbesfeld R, Cliffe A, Brabletz T, Bienz M. Nuclear export of the APC
742 tumour suppressor controls beta-catenin function in transcription. *EMBO J*.
743 2003;22(5):1101-1113.

744 49. Lu Y, Xie S, Zhang W, et al. Twa1/Gid8 is a beta-catenin nuclear retention factor
745 in Wnt signaling and colorectal tumorigenesis. *Cell Res*. 2017;27(12):1422-1440.

746 50. Henderson BR, Fagotto F. The ins and outs of APC and beta-catenin nuclear

747 transport. *EMBO Rep*. 2002;3(9):834-839.

748 51. Henderson BR. Nuclear-cytoplasmic shuttling of APC regulates beta-catenin
749 subcellular localization and turnover. *Nat Cell Biol*. 2000;2(9):653-660.

750 52. Xu L, Massague J. Nucleocytoplasmic shuttling of signal transducers. *Nat Rev*
751 *Mol Cell Biol*. 2004;5(3):209-219.

752 53. Wolff B, Sanglier JJ, Wang Y. Leptomycin B is an inhibitor of nuclear export:
753 inhibition of nucleo-cytoplasmic translocation of the human immunodeficiency virus
754 type 1 (HIV-1) Rev protein and Rev-dependent mRNA. *Chem Biol*. 1997;4(2):139-
755 147.

756 54. Kirli K, Karaca S, Dehne HJ, et al. A deep proteomics perspective on CRM1-
757 mediated nuclear export and nucleocytoplasmic partitioning. *Elife*. 2015;4.

758 55. Dimitrova YN, Li J, Lee YT, et al. Direct ubiquitination of beta-catenin by Siah-1
759 and regulation by the exchange factor TBL1. *J Biol Chem*. 2010;285(18):13507-
760 13516.

761 56. Graham TA, Weaver C, Mao F, Kimelman D, Xu WQ. Crystal structure of a β-
762 catenin/Tcf complex. *Cell*. 2000;103(6):885-896.

763 57. Rallapalli R, Strachan G, Cho B, Mercer WE, Hall DJ. A novel MDMX transcript
764 expressed in a variety of transformed cell lines encodes a truncated protein with
765 potent p53 repressive activity. *Journal of Biological Chemistry*. 1999;274(12):8299-
766 8308.

767 58. Huang CW, Chen YW, Lin YR, et al. Conditional Knockout of Breast Carcinoma
768 Amplified Sequence 2 (BCAS2) in Mouse Forebrain Causes Dendritic Malformation

769 via beta-catenin. *Sci Rep*. 2016;6:34927.

770 59. Xu Q, Wang F, Xiang Y, et al. Maternal BCAS2 protects genomic integrity in
771 mouse early embryonic development. *Development*. 2015;142(22):3943-3953.

772 60. Zhang J, Liu W, Li G, et al. BCAS2 is involved in alternative splicing and mouse
773 oocyte development. *FASEB J*. 2022;36(2):e22128.

774 61. Yamaguchi TP. Heads or tails: Wnts and anterior-posterior patterning. *Current*
775 *Biology*. 2001;11(17):R713-R724.

776 62. Kozmikova I, Kozmik Z. Wnt/β-catenin signaling is an evolutionarily conserved
777 determinant of chordate dorsal organizer. *Elife*. 2020;9.

778 63. Brafman D, Willert K. Wnt/β-Catenin Signaling during Early Vertebrate Neural
779 Development. *Developmental Neurobiology*. 2017;77(11):1239-1259.

780 64. Lickert H, Cox B, Wehrle C, Taketo MM, Kemler R, Rossant J. Dissecting
781 Wnt/β-catenin signaling during gastrulation using RNA interference in mouse
782 embryos. *Development*. 2005;132(11):2599-2609.

783 65. Morgan RG, Ridsdale J, Tonks A, Darley RL. Factors Affecting the Nuclear
784 Localization of β-Catenin in Normal and Malignant Tissue. *Journal of Cellular*
785 *Biochemistry*. 2014;115(8):1351-1361.

786 66. Neufeld KL, Nix DA, Bogerd H, et al. Adenomatous polyposis coli protein
787 contains two nuclear export signals and shuttles between the nucleus and cytoplasm.
788 *Proceedings of the National Academy of Sciences of the United States of America*.
789 2000;97(22):12085-12090.

790 67. Li FQ, Mofunanya A, Harris K, Takemaru KI. Chibby cooperates with 14-3-3 to

791 regulate β-catenin subcellular distribution and signaling activity. *Journal of Cell*
792 *Biology*. 2008;181(7):1141-1154.
793 68. Cong F, Varmus H. Nuclear-cytoplasmic shuttling of Axin regulates subcellular
794 localization of β-catenin. *Proceedings of the National Academy of Sciences of the*
795 *United States of America*. 2004;101(9):2882-2887.
796 69. Ki H, Oh M, Chung SW, Kim K. β-Catenin can bind directly to CRM1
797 independently of adenomatous polyposis coli, which affects its nuclear localization
798 and LEF-1/β-catenin-dependent gene expression. *Cell Biology International*.
799 2008;32(4):394-400.
800 70. Murillo-Garzón V, Kypta R. WNT signalling in prostate cancer. *Nature Reviews*
801 *Urology*. 2017;14(11):683-696.
802 71. Zhan T, Rindtorff N, Boutros M. Wnt signaling in cancer. *Oncogene*.
803 2017;36(11):1461-1473.
804 72. Yu FY, Yu CH, Li FF, et al. Wnt/β-catenin signaling in cancers and targeted
805 therapies. *Signal Transduction and Targeted Therapy*. 2021;6(1).
806 73. Salmerón-Hernández A, Noriega-Reyes MY, Jordan A, Baranda-Avila N, Langley
807 E. BCAS2 Enhances Carcinogenic Effects of Estrogen Receptor Alpha in Breast
808 Cancer Cells. *International Journal of Molecular Sciences*. 2019;20(4).
809 74. Wang LP, Chen TY, Kang CK, Huang HP, Chen SL. BCAS2, a protein enriched
810 in advanced prostate cancer, interacts with NBS1 to enhance DNA double-strand
811 break repair. *British Journal of Cancer*. 2020;123(12):1796-1807.
812

813 **Figures and figure legends**

814 **Figure 1**

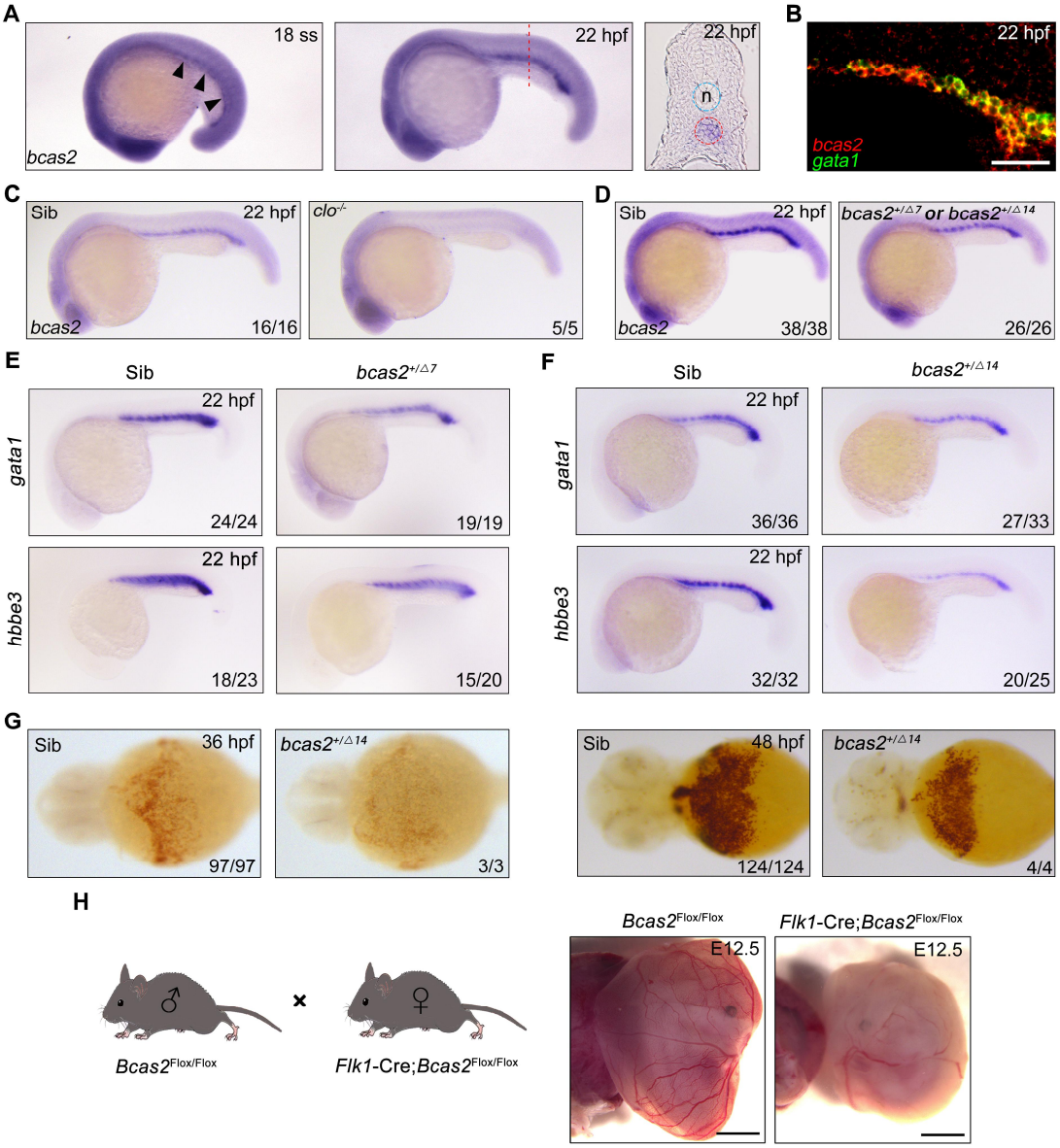

815

816

817 **Figure 1. *bcas2* is expressed in the ICM and required for primitive hematopoiesis.**
818 (A) WISH assay showing *bcas2* expression in the ICM at the 18-somite stage and 22
819 hpf. The dotted lines represent the section position and the black arrowheads indicate
820 the ICM region. n, notochord. (B) Double FISH assay showing the expression pattern
821 of *bcas2* and *gata1* in the ICM at 22 hpf. Scale bar, 50 μm. (C-D) Comparison of
822 *bcas2* expression in *cloche* mutants (C) or *bcas2* heterozygous mutants (D) along with
823 their corresponding siblings. (E-F) Expression analysis of *gata1* and *hbbe3* in
824 $bcas2^{+/\Delta 7}$ and $bcas2^{+/\Delta 14}$ embryos. (G) Hemoglobin detection using *o*-dianisidine
825 staining in *bcas2* homozygous mutant at 36 and 48 hpf. (H) Representative images of
826 yolk sac from the hemangioblast-specific *Bcas2* knockout mice and their siblings.
827 $Bcas2^{F/F}$ females were crossed with $Bcas2^{F/+}$*;Flk1-Cre* males to induce the deletion of
828 *Bcas2* in hemangioblasts. Scale bar, 1 mm.
829
830

831 **Figure 2**

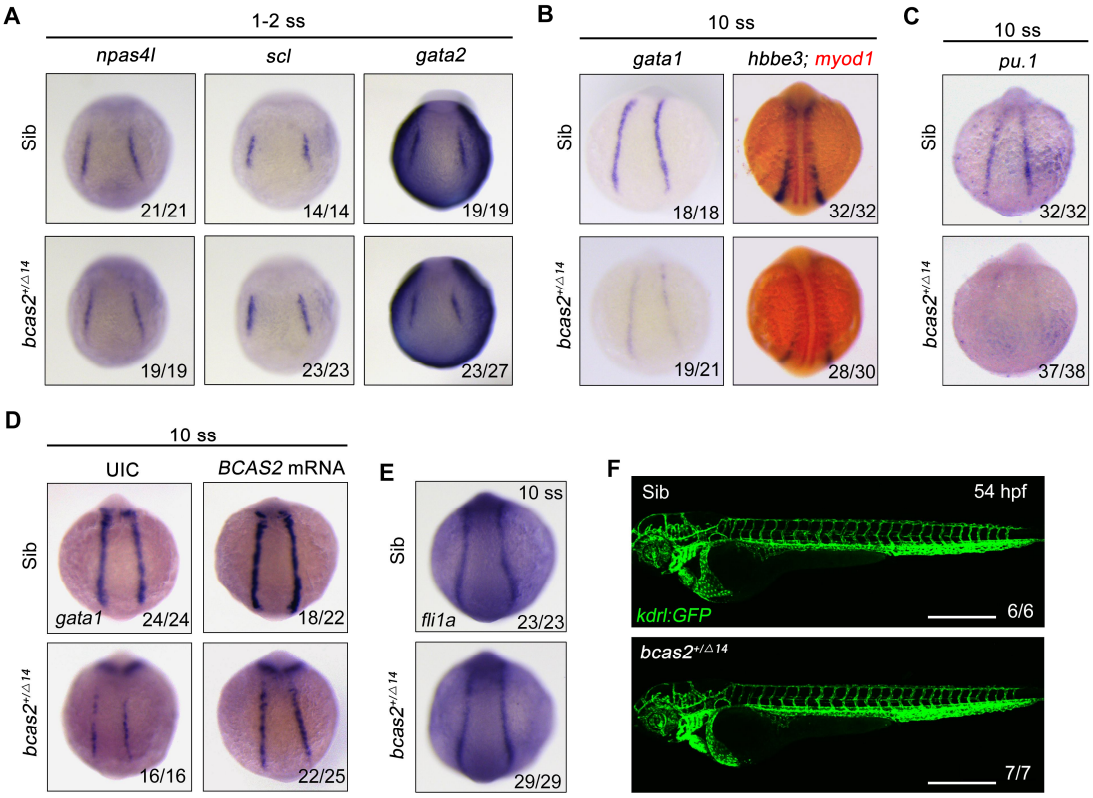

832

833

834 **Figure 2. *bcas2* is required for hematopoietic progenitor differentiation.** (A-C)
835 Expression analysis of hemangioblast markers *npas4l*, *scl, gata2* (A), erythroid
836 progenitor markers *gata1*, *hbbe3* (B), and myeloid marker *pu.1* (C) in *bcas2*$^{+/\Delta 14}$
837 embryos and their wild-type siblings at indicated stages. (D) Expression changes of
838 *gata1* in *bcas2*$^{+/\Delta 14}$ embryos overexpressing BCAS2 at the 10-somite stage. The
839 indicated embryos were injected with or without 300 pg of human *BCAS2* mRNA at
840 the one-cell stage. (E) Expression of endothelial marker *fli1a* in *bcas2*$^{+/\Delta 14}$ and sibling
841 embryos at the 10-somite stage. (G) Confocal imaging of *bcas2*$^{+/\Delta 14}$ and control
842 sibling *Tg(kdrl:GFP*) embryos at 54 hpf. Scale bar, 500 μm.
843

844 **Figure 3**

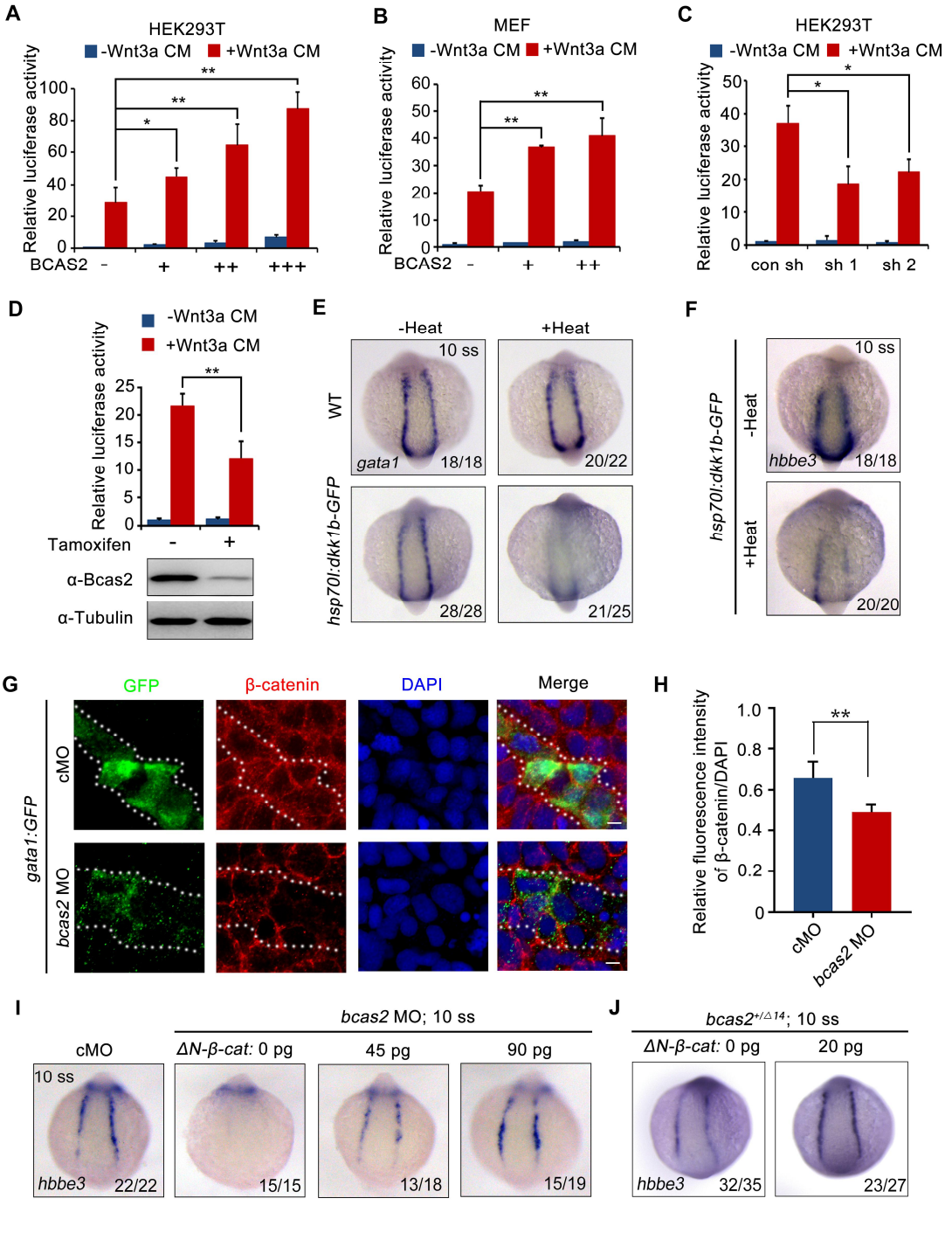

845

846

847 **Figure 3. BCAS2 promotes primitive hematopoiesis via activating Wnt signaling.**
848 (A-B) Overexpression of BCAS2 increases Wnt3a-induced TOPflash activity in
849 HEK293T cells (A) and MEFs (B). Different amounts of plasmid expressing BCAS2
850 (0, 80, 160, or 320 ng/well) were transfected into cells, together with the super-
851 TOPflash luciferase and Renilla luciferase vectors. After 36 h of transfection, cells
852 were treated with or without Wnt3a CM for 12 h and harvested for luciferase assays.
853 $*P < 0.05$; $**P < 0.01$ (Student's *t-test*). (C) The Wnt3a-induced TOPflash activity is
854 decreased in BCAS2-deficient cells. HEK293T Cells were transfected with shRNA
855 plasmids, along with indicated plasmids, and harvested for luciferase reporter assay.
856 $*P < 0.05$ (Student's *t-test*) (D) *Bcas2*-cKO MEFs prepared from $Bcas2^{F/F}$ mouse
857 embryos were incubated in medium containing 100 μM tamoxifen for 72 h and then
858 subjected to western blotting and luciferase reporter assay. $**P < 0.01$ (Student's *t-*
859 *test*). (E-F) Expression analysis of *gata1* (E) and *hbbe3* (F) in *Tg(hsp70l:dkk1b-GFP)*
860 embryos after heat shock at 16 hpf. (G-H) Immunofluorescence staining of β-catenin
861 in *Tg(gata1:GFP)* embryos at 16 hpf. The embryos were injected with 8 ng of the
862 indicated MO at the one-cell stage. The dotted lines show the GFP-positive
863 hematopoietic progenitor cells. Scale bars, 5 μm. The relative fluorescence intensity
864 of nuclear β-catenin was quantified in (H). $**P < 0.01$ (Student's *t-test*). (I-J)
865 Expression of *hbbe3* in *bcas2* morphants (I) and $bcas2^{+/\Delta 14}$ mutants (J) overexpressing
866 ΔN-β-catenin. Embryos were injected with the indicated MO together with *ΔN-β-*
867 *catenin* mRNA at the one-cell stage and harvested at the 10-somite stage for *in situ*
868 hybridization.

869 **Figure 4**

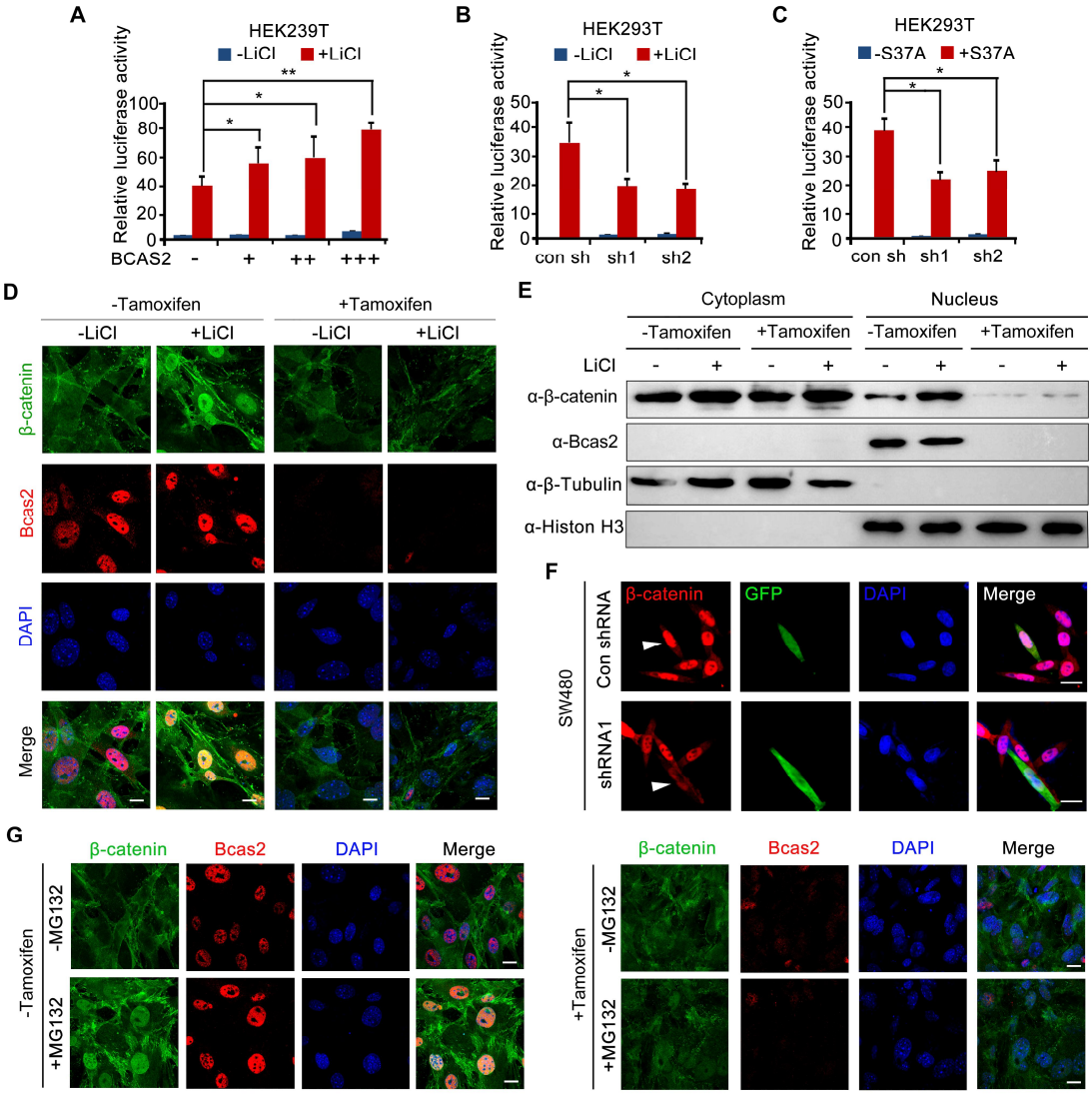

870

871

872 **Figure 4. BCAS2 is essential for β-catenin nuclear accumulation.** (A-C) BCAS2
873 enhances LiCl-induced TOPflash activity in HEK293T cells. Cells were transfected
874 with BCAS2 expression plasmids (A), shRNA plasmids (B), or S37A-β-catenin
875 expression plasmids (C), together with the TOPflash luciferase and Renilla luciferase
876 vectors. After transfection, cells were subsequently treated with or without 100 ng/mL
877 LiCl for 12 h and assayed for luciferase activity. $^{*}P < 0.05$; $^{**}P < 0.01$ (Student's *t-*
878 *test*). (D-E) *Bcas2*-cKO MEFs were incubated with tamoxifen for 24 h and then
879 treated with or without 100 ng/mL LiCl. The nuclear accumulation of β-catenin was
880 analyzed using immunofluorescence (D) and western blotting (n=3) (E) Scale bars, 10
881 μm. (F) SW480 cells were transfected with the indicated shRNA constructs, and the
882 endogenous β-catenin protein was detected using immunofluorescence 48 h after
883 transfection. The expression of GFP served as a transfection control. The arrowheads
884 indicate the cells transfected with indicated shRNA constructs. Scale bars, 10 μm. (G)
885 *Bcas2*-cKO MEFs were cultured in the presence of tamoxifen for 24 h and then
886 treated with 20 μM MG132 for 6 h. The expression of BCAS2 and β-catenin was
887 measured by immunofluorescence. Scale bars, 10 μm.
888

889 **Figure 5**

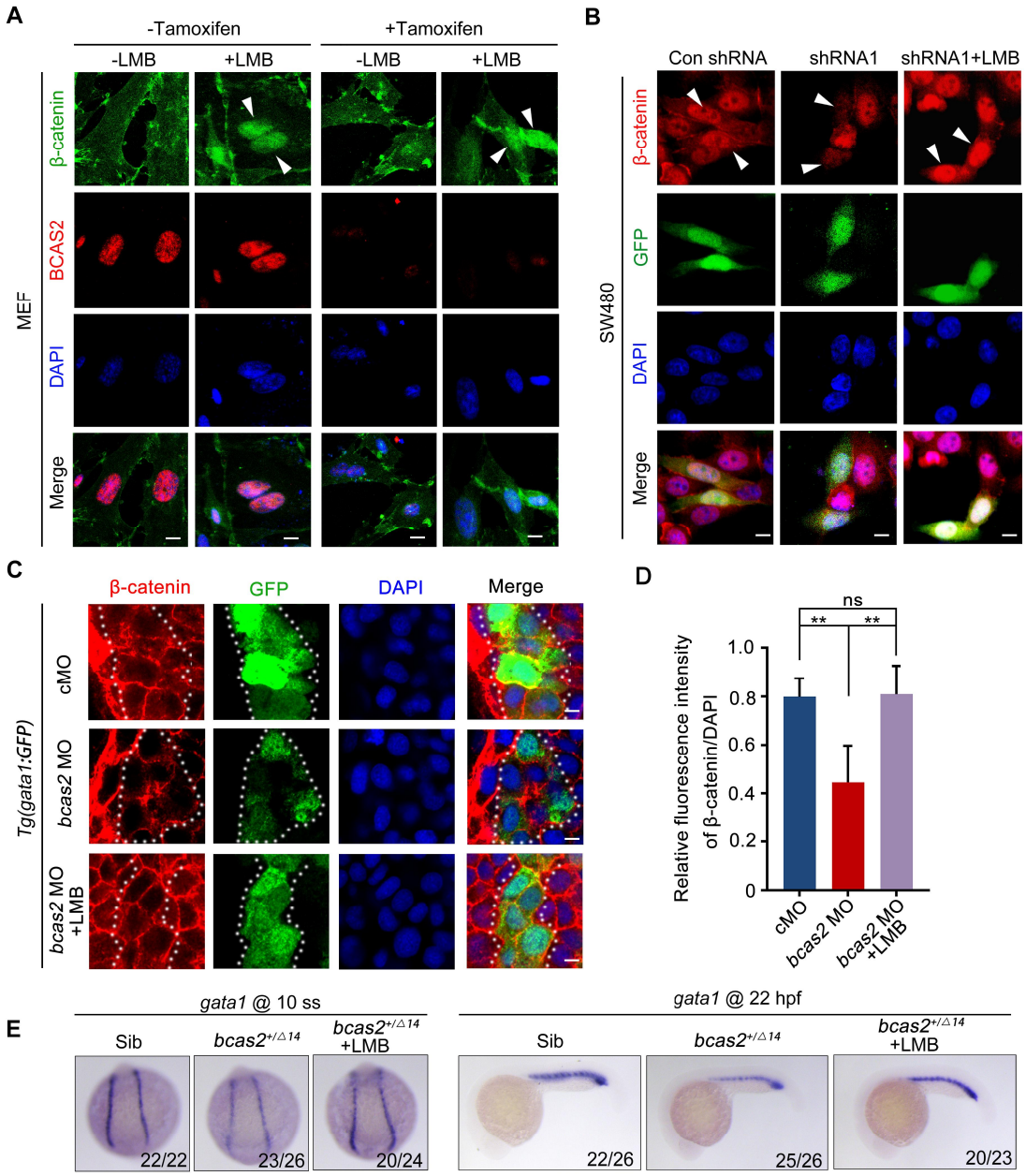

890

891

892 **Figure 5. BCAS2 functions in CRM1-mediated nuclear export of β-catenin.** (A)
893 Tamoxifen-treated *Bcas2*-cKO MEFs were incubated with 20 nM LMB for 3 h. The
894 expression of Bcas2 and β-catenin was analyzed using immunofluorescence. The
895 arrowheads show the cells with nuclear β-catenin accumulation. Scale bars, 10 μm. (B)
896 SW480 cells were transfected with the indicated shRNA constructs and then treated
897 with LMB for 3 h before immunostaining. GFP was regarded as a transfection control.
898 The arrowheads indicate the transfected cells. Scale bars, 10 μm. (C-D)
899 Immunofluorescence staining of β-catenin in *bcas2* morphants with *Tg(gata1:GFP)*
900 background at 16 hpf. Embryos were exposed to 20 nM LMB from the bud stage. The
901 dotted lines indicate the GFP-positive hematopoietic progenitor cells. Scale bars, 5
902 μm. The relative fluorescence intensity of nuclear β-catenin was quantified in (D). ns,
903 not significant; $^{**}P < 0.01$ (Student's *t-test*). (E) *bcas2*$^{+/\Delta 14}$ embryos were treated with
904 20 nM LMB for 6 h and then subjected to WISH assay to analyze the expression of
905 *gata1* at the indicated stages.
906

907 **Figure 6**

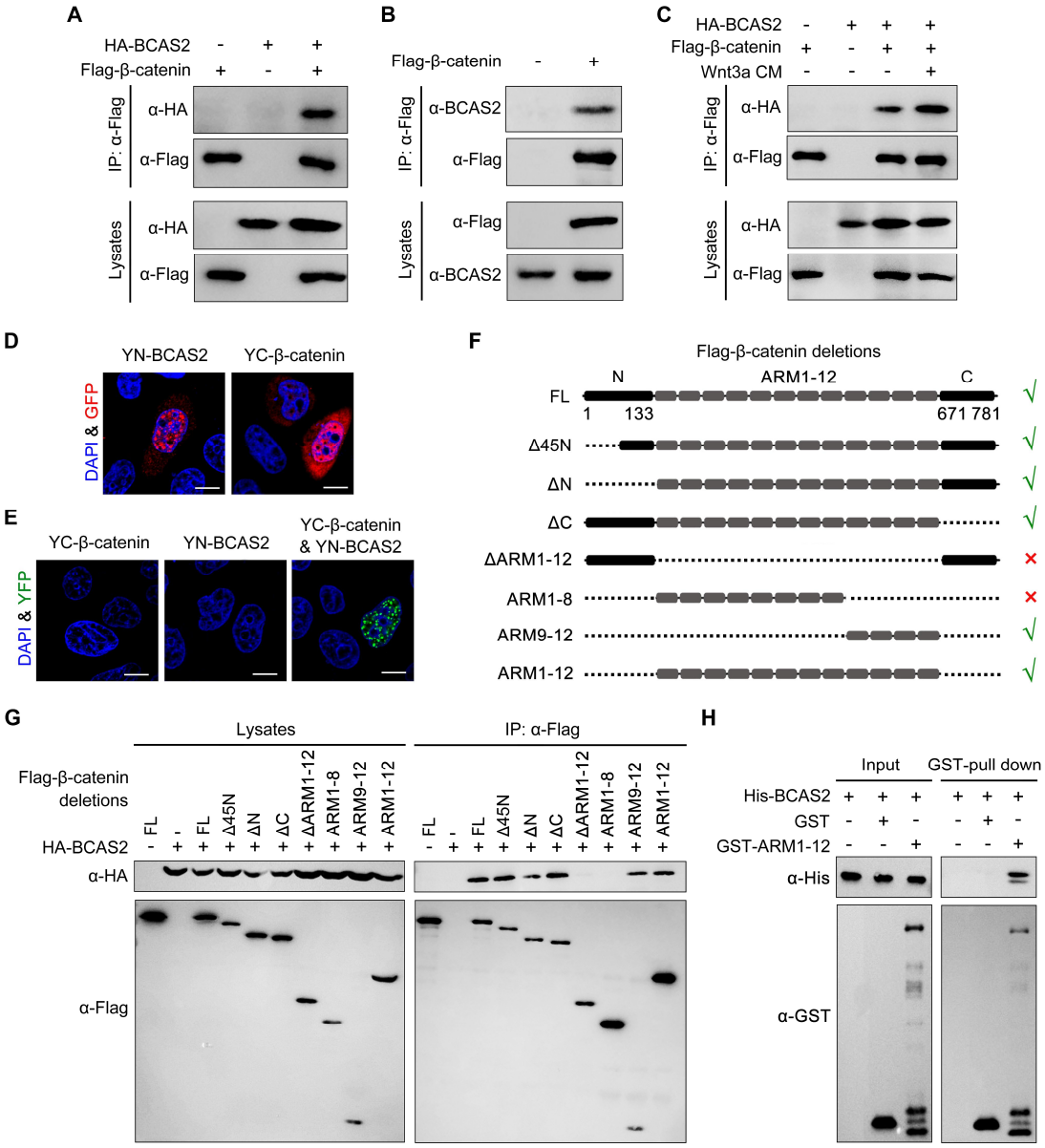

908

909

910 **Figure 6. BCAS2 interacts with β-catenin.** (A-C) Flag-tagged β-catenin was co-
911 transfected with or without HA-tagged BCAS2 into HEK293T cells. Cell lysates were
912 immunoprecipitated using anti-Flag antibody. Eluted proteins were analyzed by
913 western blotting using indicated antibodies. In panel C, for Wnt signaling activation,
914 cells were treated with Wnt3a CM for 5 h before harvest. (D-E) YN-BCAS2 and YC-
915 β-catenin were either individually or collectively transfected into HeLa cells. The
916 expression of YN-BCAS2 and YC-β-catenin was analyzed with anti-GFP antibody
917 (D). The reconstituted YFP fluorescence in living cells was detected by confocal laser
918 scanning microscopy with excitation at 488 nm (E). Scale bars, 10 μm. (F)
919 Schematics of full-length and deletion mutants of β-catenin. (G) HEK293T cells were
920 transfected with HA-tagged BCAS2 and Flag-tagged deletion mutants of β-catenin.
921 Cell lysates were then immunoprecipitated using anti-Flag antibody followed by
922 western blot analysis. (H) GST pull-down assays were performed using bacterially
923 expressed GST, GST-ARM1-12, and His-BCAS2.
924

925 **Figure 7**

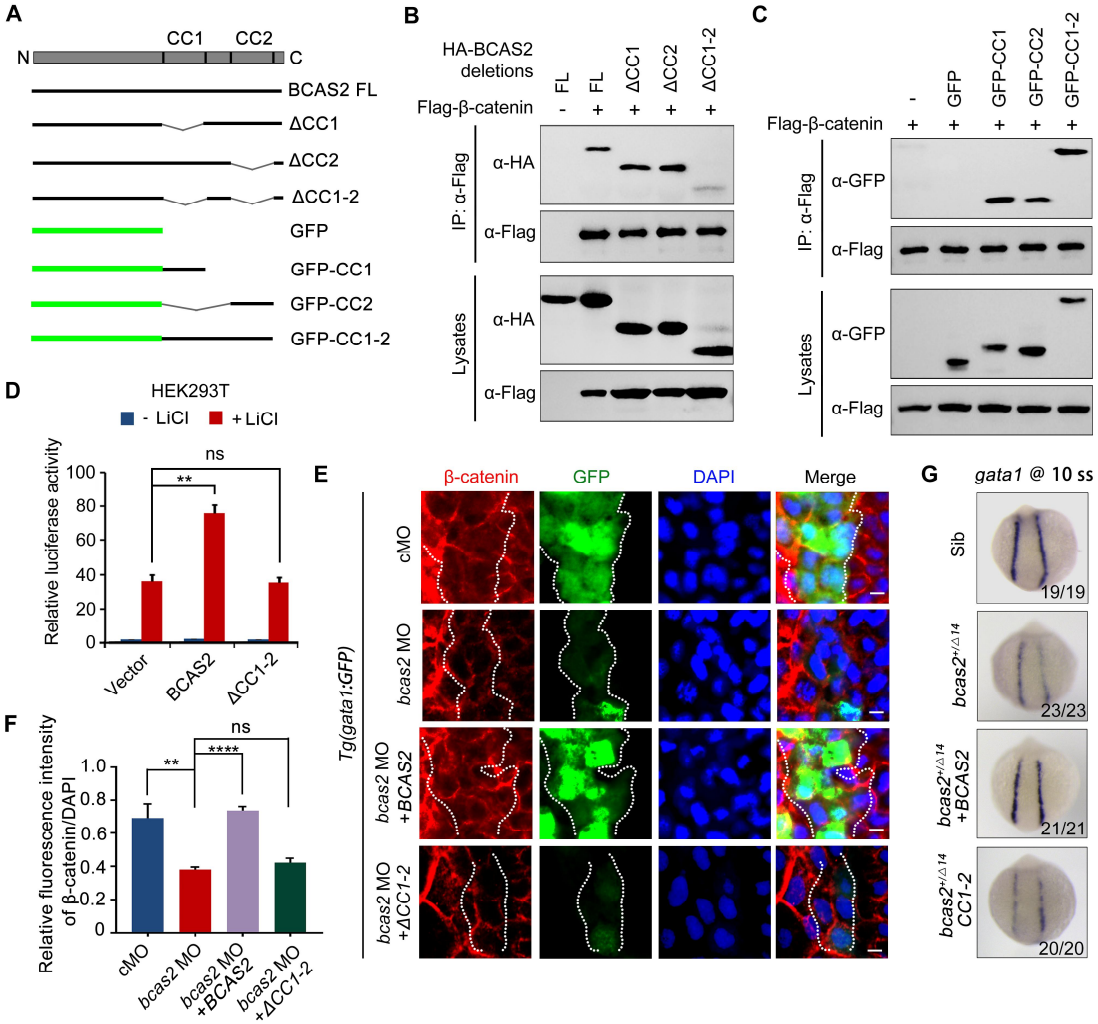

926

927

928 **Figure 7. BCAS2 sequesters β-catenin in the nucleus via its CC domains.** (A)
929 Schematics of full length and deletion mutants of BCAS2. (B-C) HEK293T cells were
930 transfected with Flag-β-catenin and indicated deletion mutants of BCAS2. Cell lysates
931 were subjected to immunoprecipitation with anti-Flag antibody. Eluted proteins were
932 immunoblotted using anti-HA (B) or anti-GFP antibodies (C) for BCAS2 detection.
933 (D) HEK293T cells transfected with the indicated plasmids were treated with 100
934 ng/mL LiCl for 12 h, and then subjected to luciferase assay. Note that overexpression
935 of BCAS2 without the CC domains failed to increase LiCl-induced TOPflash activity.
936 Data represent the mean ± SD of three independent experiments. ns, not significant;
937 $^{**}P < 0.01$ (Student's *t-test*). (E-F) Immunofluorescence staining of β-catenin in
938 *Tg(gata1:GFP)* embryos at 16 hpf. The embryos were injected with 8 ng *bcas2* MO
939 and 300 pg of full length *BCAS2* mRNA or *ΔCC1-2* mRNA at the one-cell stage.
940 Scale bars, 5 μm. The relative fluorescence intensity of nuclear β-catenin was
941 quantified in (F). ns, not significant; $^{**}P < 0.01$; $^{****}P < 0.0001$ (Student's *t-test*). (G)
942 Transcripts of *gata1* were evaluated by WISH in *bcas2*$^{+/\Delta 14}$ embryos injected with 300
943 pg of *BCAS2* mRNA or *ΔCC1-2* mRNA.
944

945 **Supplemental figures**

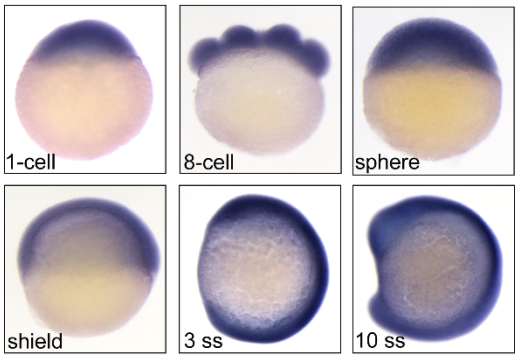

946

947 **Figure S1. Expression patterns of *bcas2* in wild-type embryos during**

948 **development.** Expression of *bcas2* in wild-type embryos at the indicated

949 developmental stages was analyzed using whole-mount *in situ* hybridization.

950

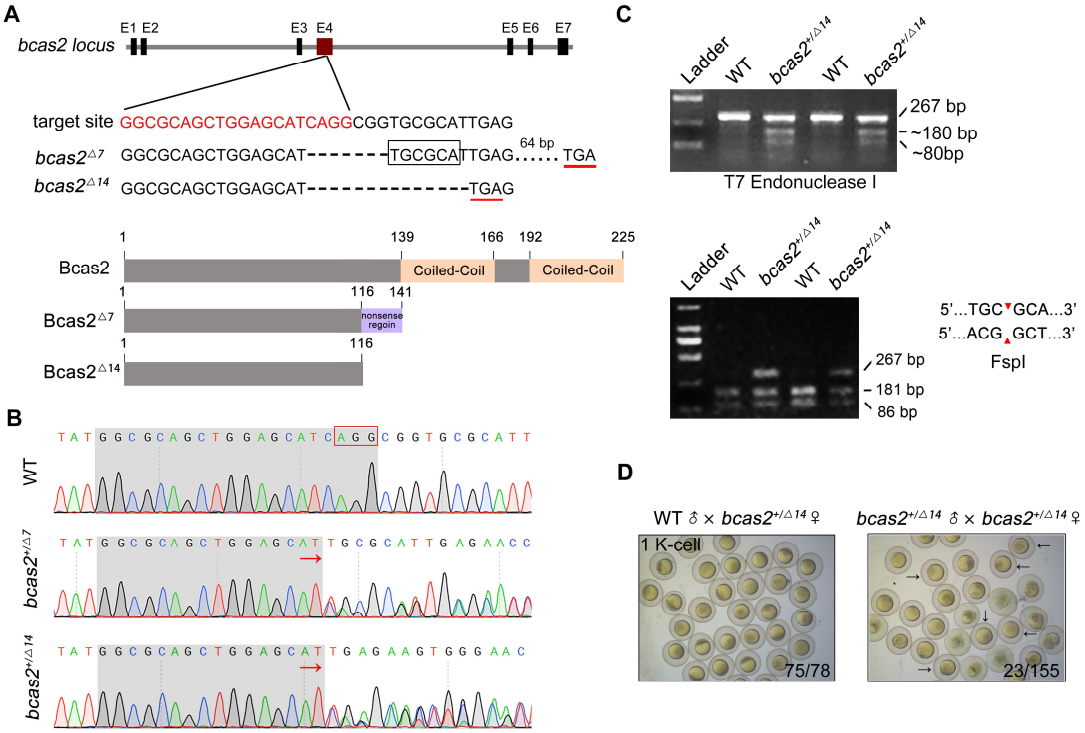

Figure S2. Zebrafish *bcas2* mutants are generated by using CRISPR/Cas9 system. (A) Schematic showing generation of *bcas2* mutants. Two mutant lines were obtained with mutations that resulted in premature translation termination, resulting in truncated Bcas2 proteins lacking the C-terminal CC domains. (B) Identification of *bcas2* mutations using DNA sequencing. (C) The *bcas2*$^{+/\Delta 7}$ and *bcas2*$^{+/\Delta 14}$ mutants were identified via T7 endonuclease (the upper panel) or FspI restriction enzyme (the lower panel) digestions. (D) Bright field images of embryos derived from crossing indicated females with heterozygous male mutants. Black arrows refer to the embryos that exhibited an abnormal cleavage. The ratio of viable embryos was indicated.

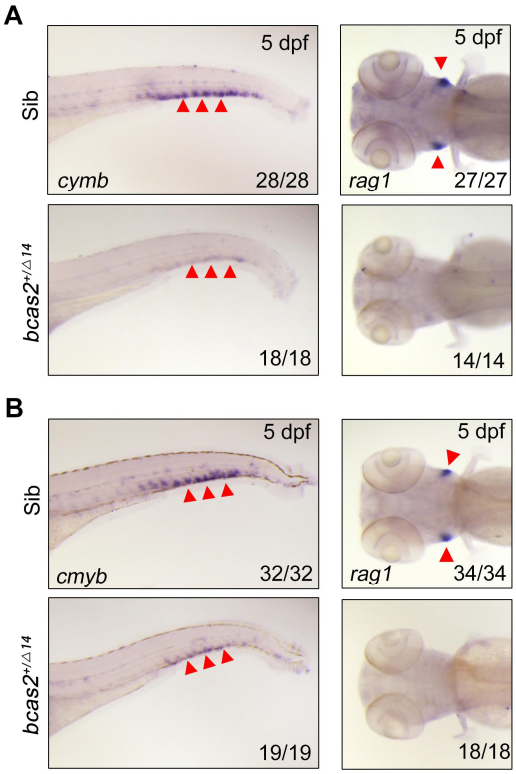

Figure S3. *bcas2* is essential for definitive hematopoiesis. (A-B) Expression changes of *cymb* and *rag1* in *bcas2*$^{+/\Delta 7}$ (A) and *bcas2*$^{+/\Delta 14}$ (B) embryos compared with their siblings. Arrowheads on the left panels indicate the caudal hematopoietic tissue, and those on the right panels indicate the thymus.

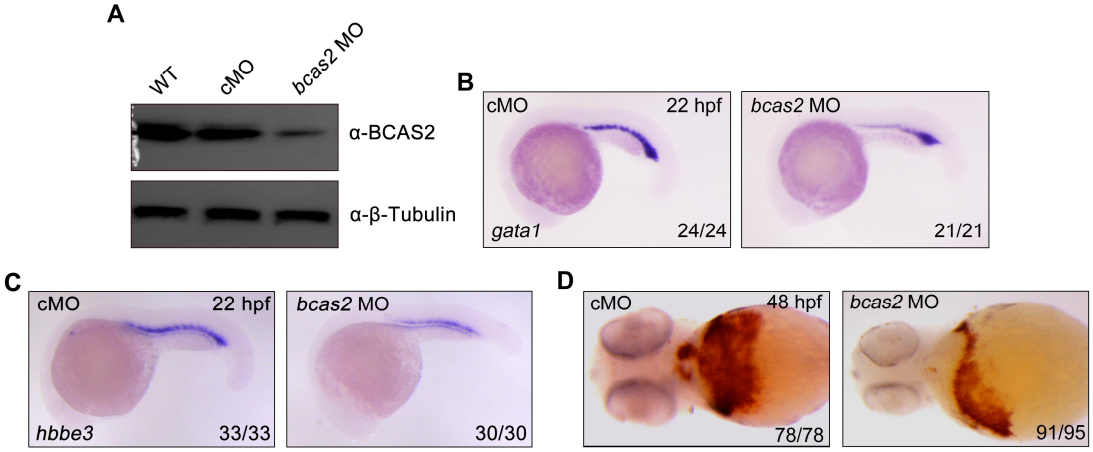

Figure S4. Knockdown of *bcas2* impairs primitive hematopoiesis. (A) Western blot analysis showing the expression changes of Bcas2 protein in wild-type embryos and embryos injected with 8 ng control MO (cMO) or *bcas2* MO. (B-C) Expression of *gata1* (B) and *hbbe3* (C) in *bcas2* morphants and control embryos. (D) Detection of hemoglobin levels by *o*-dianisidine staining in *bcas2* morphants and control embryos.

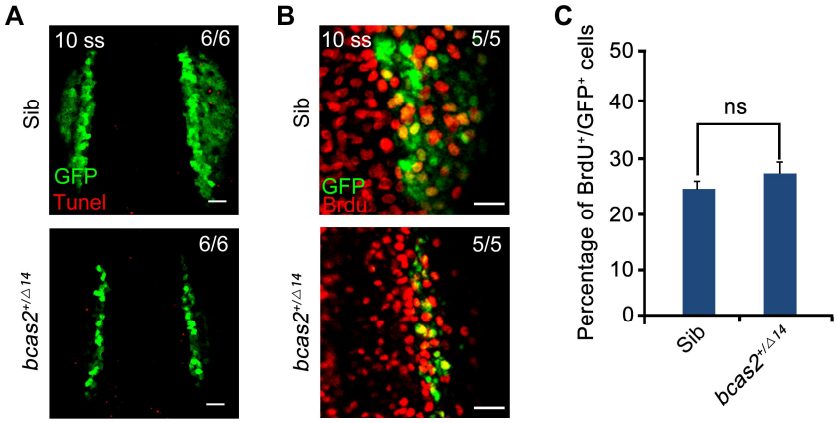

984

985 **Figure S5. *bcas2* is dispensable for the survival and proliferation of**

986 **hematopoietic cells.** (A) Cell apoptosis was detected by TUNEL assay in *bcas2*$^{+/\Delta 14}$

987 embryos and their siblings with *Tg(gata1:GFP)* background. Scale bar, 50 μm. (B-C)

988 Cell proliferation was detected by BrdU staining in *bcas2*$^{+/\Delta 14}$ embryos and their

989 siblings with *Tg(gata1:GFP)* background. Scale bars, 20 μm. The percentage of

990 BrdU^{+}/GFP^{+} cells (% over the total number of GFP^{+} cells) was quantified from six

991 embryos in each group (C). Data represent the mean ± SD of three independent

992 experiments. ns, not significant (Student's *t-test*).

993

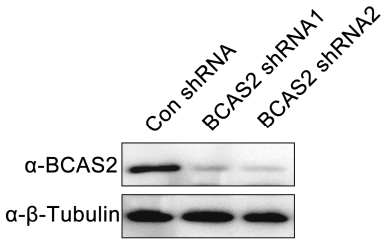

994

995 **Figure S6. Western blot analysis of HEK293T Cells transfected with**

996 **corresponding shRNA constructs.**

997

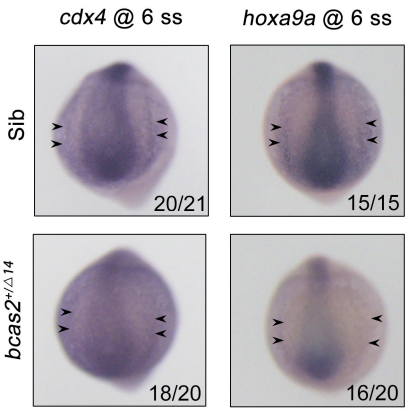

Figure S7. Expression patterns of *cdx4* and *hoxa9a* in *bcas2*$^{+/\Delta 14}$ embryos and their siblings at the 6-somite stage. Black arrows indicate the posterior lateral mesoderm.

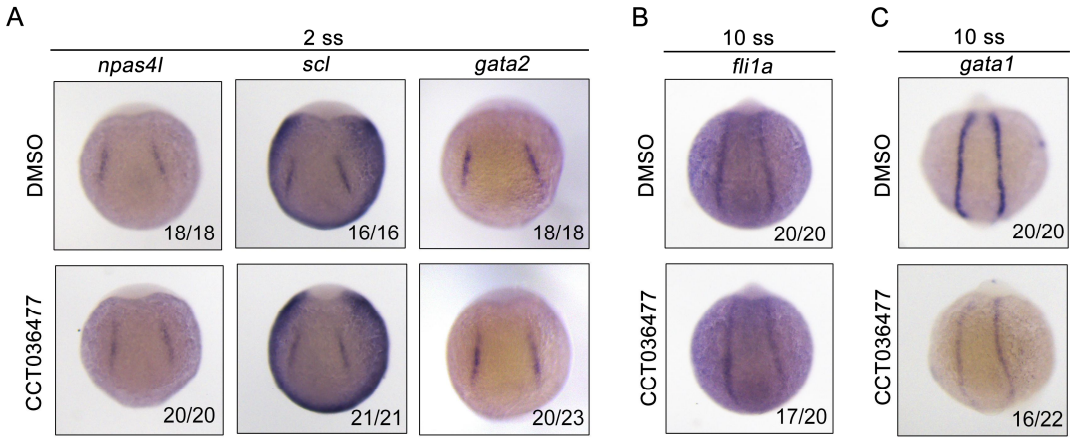

1003

1004 **Figure S8. Inhibition of Wnt signaling does not affect the generation of**

1005 **hemangioblasts or their endothelial differentiation, but impairs their**

1006 **hematopoietic differentiation.** Expression of hemangioblast markers *npas4l*, *scl*,

1007 *gata2* (A), endothelial marker *fli1a* (B) and erythroid progenitor marker *gata1* (C) at

1008 the indicated stages. Wild-type embryos were treated with 10 μM CCT036477 from 9

1009 hpf and then collected for whole-mount *in situ* hybridizations.

1010

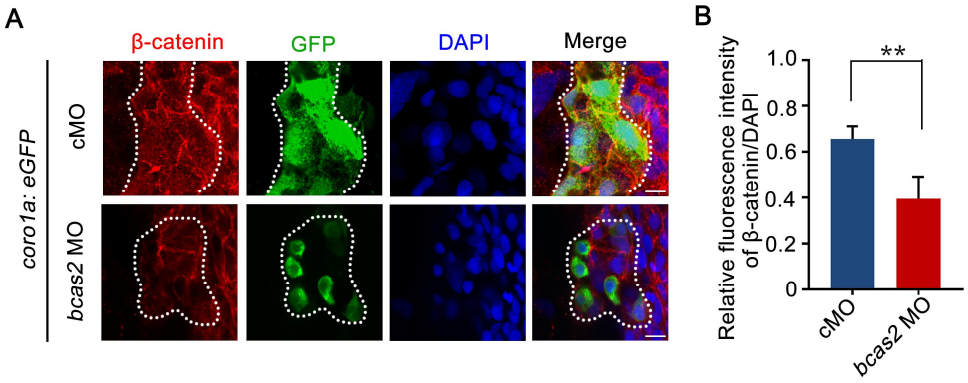

1011

1012 **Figure S9. Knockdown of *bcas2* significantly reduces nuclear β-catenin in the**

1013 **primitive myeloid cells.** Immunofluorescence staining of β-catenin in

1014 *Tg(coro1a:GFP)* embryos at 17 hpf. The embryos were injected with 8 ng of the

1015 indicated MOs at the one-cell stage and then collected for immunofluorescence

1016 staining. The dotted lines refer to the GFP-positive primitive myeloid cells. Scale bars,

1017 10 μm. The relative fluorescence intensity of nuclear β-catenin was quantified in (B).

1018 $^{**}P < 0.01$ (Student's *t-test*).

1019

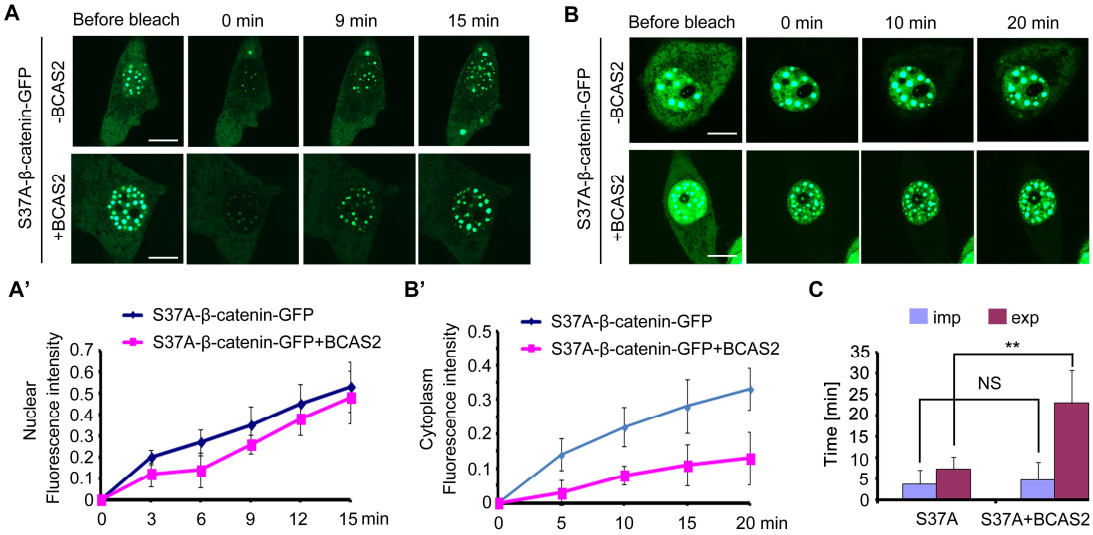

1020

1021 **Figure S10. BCAS2 inhibits the nuclear export of β-catenin.** (A-B') GFP-tagged
1022 S37A-β-catenin was co-expressed with or without BCAS2 in HeLa cells. The entire
1023 nucleus (A) or entire cytoplasm (B) was bleached. (A-A') Representative images at
1024 the indicated timepoints showing the kinetics of nuclear import of S37A-β-catenin are
1025 shown in (A) and the related fluorescence recovery curves are shown in (A'). Time-
1026 lapse imaging (B) and recovery curves (B') from cytoplasmic photobleaching
1027 experiments showed the kinetics of nuclear export of S37A-β-catenin. Scale bars, 10
1028 μm. (C) Quantitative analysis of fluorescence recoveries after photobleaching (n=7).
1029 Data represent the mean ± SD of three independent experiments. Student's t-test was
1030 used. ns, not significant, $^{**}P < 0.01$ (Student's *t-test*).

1031

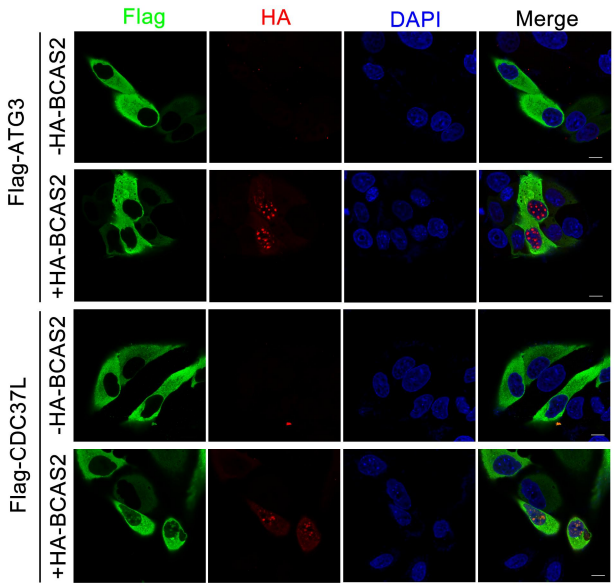

Figure S11. Overexpression of BCAS2 slightly enhances the nuclear accumulation of CDC37L, and has no influence on the distribution of ATG3. HeLa cells were transfected with the indicated plasmids and then subjected to immunostaining using anti-Flag and anti-HA antibodies. The nuclei were labeled with DAPI. Scale bar, 10 μm.

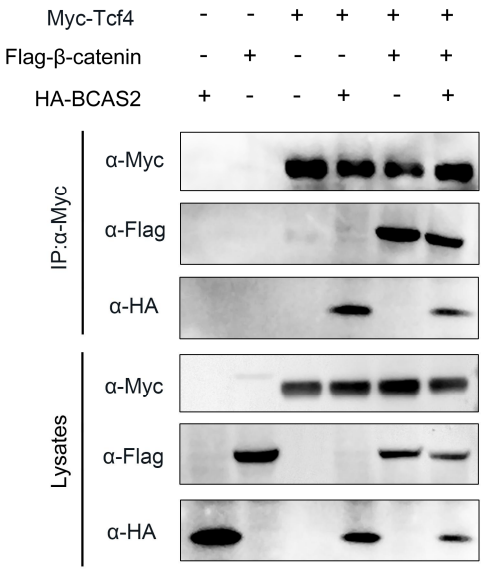

1039

1040 **Figure S12. The interaction between β-catenin and TCF4 remains unaffected in**

1041 **the presence of BCAS2.** HEK293T cells were transfected with the indicated

1042 constructs. Cell lysates were immunoprecipitated using anti-c-Myc antibody and the

1043 eluted proteins were analyzed by western blotting.

1044

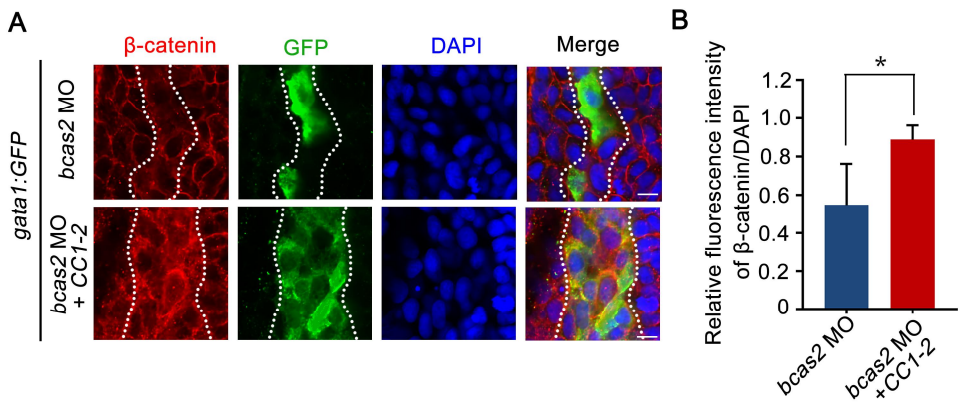

1045

1046 **Figure S13. Overexpression of the CC domains of BCAS2 restores nuclear β-**

1047 **catenin accumulation in *bcas2* morphants.** Immunofluorescence staining of β-

1048 catenin in *Tg(gata1:GFP)* embryos at 16 hpf. The embryos were injected with 8 ng

1049 *bcas2* MO and 300 pg of *BCAS2 CC1-2* mRNA at the one-cell stage. The dotted lines

1050 show the GFP-positive hematopoietic progenitor cells. Scale bars, 10 μm. The relative

1051 fluorescence of nuclear β-catenin was quantified in (B). *$P < 0.05$ (Student's *t-test*).

1052

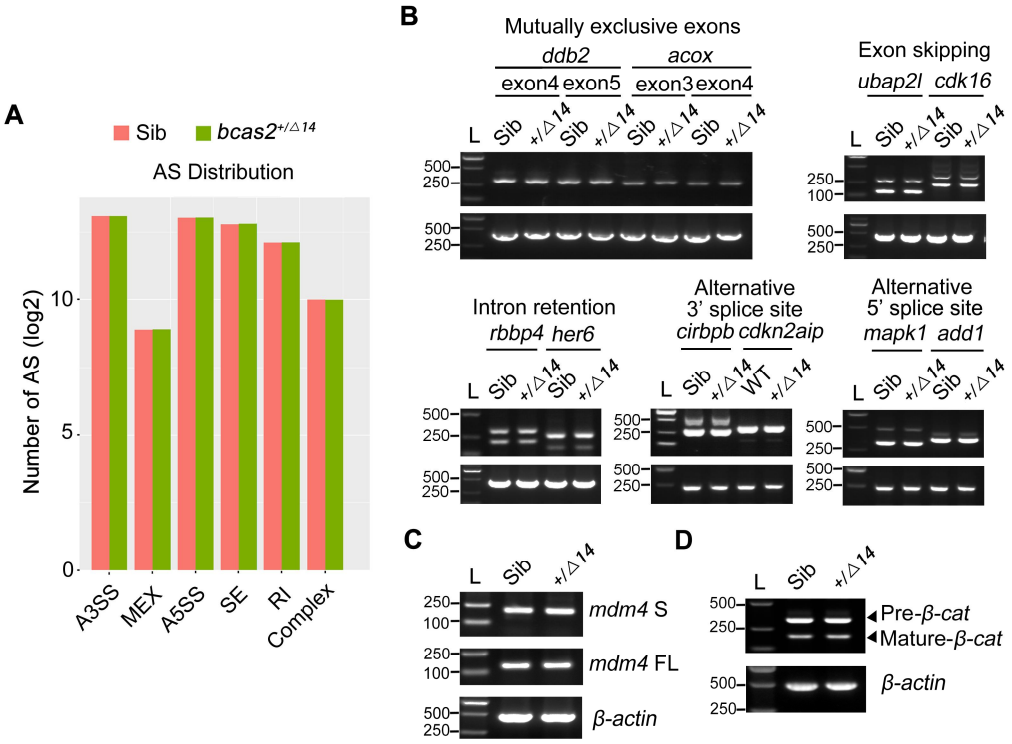

1053

1054 **Figure S14. Haploinsufficiency of *bcas2* does not affect pre-mRNA splicing**
1055 **during primitive hematopoiesis.** (A) The number of five major types of alternative
1056 splicing events was analyzed from RNA sequencing data. Embryos were lysed at the
1057 10-somite stage and subjected to reverse transcription. The cDNA library was
1058 prepared, sequenced and then analyzed using rMATS. The five main alternative
1059 splicing types refer to exon skipping (SE), alternative 3' splicing site (A3SS),
1060 alternative 5' splicing site (A5SS), intron retention (RI), and mutually exclusive exons
1061 (MEX). (B) Examples of different types of alternative splicing were analyzed by
1062 reverse transcription PCR using total RNA from sibling and *bcas2*$^{+/\Delta 14}$ embryos at the
1063 10-somite stage. (C) Reverse transcription PCR analysis of total *mdm4*-FL and *mdm4*-
1064 S isoforms in *bcas2*$^{+/\Delta 14}$ and sibling embryos at the 10-somite stage. (D) Analysis the
1065 pre-mRNA and mature mRNA of *β-catenin* in *bcas2*$^{+/\Delta 14}$ and sibling embryos at the

1066 10-somite stage.

1067

1068 **Supplemental Table 1**

1069 **Primers Used for Genotyping**

Strain	Directions	Sequence (5' to 3')
Flk1-Cre mouse	Forward	CGGTTATTCAACTTGCACCAC
	Reverse	CAGGACTGAAAGCCCAGACT
Bcas2$^{Flox/Flox}$ mouse	Forward	ATTCCAGCAGTTGGTGTGGG
	Reverse	CATTGCTGGACAGAAGGTGAG
Flk1-Cre;*Bcas2*$^{Flox/Flox}$ mouse	Forward	AGGTGTATGAATGCCTGAACAAG
	Reverse	CATTGCTGGACAGAAGGTGAG
bcas2 knockout zebrafish	Forward	TGCACATACAGTAATAGGCTTACCC
	Reverse	GTCTGATTTGCATCAAAAGATGTGA

1070

1071 **Supplemental Table 2**

1072 **Primers Used for Reverse Transcription-PCR**

Symbol	Directions	Sequence (5' to 3')
ddb2	Forward	CGCTCACTTAAATCTTACAAGCTGC
	Reverse	AGTCTGGGGTACGAGACAATATCT
	Reverse	TTGGCAAAGACTTGTATAACGGATC
acox	Forward	ATCCAGATTTCCAACATGAAGACCT
	Reverse	AGGTGCCTAACATATGGAATGACTC
	Forward	TTCTCTCTCGAAGTGAGCGATATGA
	Reverse	TCTGTGCGTAGGTGCCAATAATCTC
ubap2l	Forward	GAATGTTGGTGTCAATGCATCAGCT
	Reverse	CTGCGTCTTTGTGTAAACAGAGCCT
cdk16	Forward	ATGAGGAAGATCAAACGGCAGCTGT
	Reverse	AAATTTTGCGACCGGGGTTGTTTCT
rbbp4	Forward	TGGGACACTCGTTCCAATAACACAT
	Reverse	CTGGAAGATTTCATCTTTGTGCGAC
her6	Forward	GGAGAAAAGAAGAAGAGCGAGAATC
	Reverse	GCTGCATGTTTCTGAGATGTTTCAC
cirbpb	Forward	TCCTACAGAGACGGTTACGACAGTT
	Reverse	CCTCACCAGGCTTGAAACTCTTACA
cdkn2aip	Forward	TCGCTAATGAGGACTTGTCTTTGGA
	Reverse	ATTTATCTTGTCCATCACACGCTGC
mapk1	Forward	GTCTGTTGGTTGTATTCTGGCTGAG
	Reverse	AGGATCATAGTACTGCTCCAGGTAC
add1	Forward	AGGATGCTGGATAATCTGGGCTACA
	Reverse	GTTGCGCATCTCTTGGACTTCTTTC
Mdm4-FL	Forward	GGTCAGGTGTCCAGTGAGTCAATAA
	Reverse	AAACCATCTGAGGAGTCTTCATCTG
Mdm4-S	Forward	GAAGATCCTGGTCAGACTCCTCAGA
	Reverse	CGGGAGAGAGTTGATTGGTGTGAAT
β-catenin	Forward	GATGACGATGTGGATAATCAGGTGC
	Reverse	GAACTGTGTGGAAGGTATCTGCATG
	Forward	GGAGACAATTTCTCATTATTCTGGC
	Reverse	TCAGTAGTTTGGTGAGCTCTGGAAT
β-actin	Forward	ATGGATGATGAAATTGCCGCAC
	Reverse	ACCATCACCAGAGTCCATCACG

1073